NOTICE

The quality of this microform is heavily dependent upon the quality of the original thesis submitted for microfilming. Every effort has been made to ensure the highest quality of reproduction possible.

If pages are missing, contact the university which granted the degree.

Some pages may have indistinct print especially if the original pages were typed with a poor typewriter ribbon or if the university sent us an inferior photocopy.

Reproduction in full or in part of this microform is governed by the Canadian Copyright Act, R.S.C. 1970, c. C-30, and subsequent amendments.

AVIS

La qualité de cette microforme dépend grandement de la qualité de la thèse soumise au microfilmage. Nous avons tout fait pour assurer une qualité supérieure de reproduction.

S'il manque des pages, veuillez communiquer avec l'université qui a conféré le grade.

La qualité d'impression de certaines pages peut laisser à désirer, surtout si les pages originales ont été dactylographiées à l'aide d'un ruban usé ou si l'université nous a fait parvenir une photocopie de qualité inférieure.

La reproduction, même partielle, de cette microforme est soumise à la Loi canadienne sur le droit d'auteur, SRC 1970, c. C-30, et ses amendements subséquents.

ISBN 0-315-53793-0

AB_2C_4 Semiconducting Compounds : Crystal Growth, Intrinsic Defects And Optical Properties

By

Mostefa Golea

Thesis submitted to the
School of Graduate Studies
in partial fulfillment of the requirements
for the degree of
Master of Science in Physics

DEPARTMENT OF PHYSICS
UNIVERSITY OF OTTAWA
Ottawa, Canada
July, 1988

Contents

Acknowledgements

I would like to express my sincere gratitude to my supervisor, professor Pierre Bernard, for giving me the opportunity to work with him and for his assistance, invaluable guidance, encouragement and patience throughout the course of this work. I have benefited from his great competence not only in the field of semiconductors but also in many other fields of physics. I would like to thank Dr. E. Fortin for suggesting in part the subject and for helpful discussions. I would like to thank Dr. G. Lamarche for his friendship and encouragement.

Thanks are due to my Algerian friends who helped me with the use of computing facilities at the university.

Special thanks go to my friends, M. Boucekkine, his wife Mounira, L. Tamrabet and D.Rhoda for their encouragement.

Finally, I would like to thank my family for putting up with my absence and for their moral support.

Abstract

A critical review of the literature of AB_2C_4 compounds is presented. The application of Bridgman-Stockbarger technique to the growth of single crystals of ternary compound $CdIn_2S_4$ is described in details. Single crystals of good optical quality have been prepared by this method. The Absorption spectra of $CdIn_2S_4$ have been measured at room temperature and liquid N_2 temperature and the results indicate that this compound has an indirect-allowed transition at 2.02 ev and a direct-allowed transition at 2.41 ev (at R.T.). The absorption tail below the fundamental absorption edge has been analyzed and related to the form of trap distribution below the conduction band. A thermodynamic approach based on the influence of deviation from ideal composition on the properties of crystals is used to establish the predominant intrinsic defects in AB_2C_4 compounds. The reasons which make it difficult to control the type of conduction in these materials are discussed. Finally, a study of changes in linear susceptibility with substitutional variations of isoelectronic elements in non-metallic compounds is given. The general trend observed in these changes may be useful for practical application of the multinary materials.

La litterature concernant les composés AB_2C_4 est passée en revue afin de souligner les problèmes et les désaccords. L'application de la technique de Bridgman-Stockbarger à la croissance des cristaux du composé ternaire $CdIn_2S_4$ est décrite en details. Des cristaux de bonne qualité optique furent preparés par cette méthode.

Le spectre d'absorption du $CdIn_2S_4$ est mesuré aux temperatures T = 300K et T = 80K, et l'analyse des résultats indique que ce composé possède une transition indirecte-permise a 2.02 ev et une transition directe-permise a 2.41 ev (T = 300K). Le spectre d'absorption aux énergies inférieures à la bande interdite est analysé et interprété en fonction de la distribution des trappes sous la bande de conduction. Une approche thermodynamique basée sur l'influence des déviations de la composition parfaite des crystaux est utilisée pour prédire les défauts intrinsèques dominants dans les composés de type AB_2C_4. Les raisons qui font en sorte qu'il est difficile de controler le type de conduction dans ces matériaux sont discutées. Finalement, on presente une étude sur les changements de susceptibilité lineaire lors de substitution isoélectronique dans les composés non-métalliques. Les tendances observées pour ces changements peuvent être utiles pour les applications pratiques des composés ternaires ou quaternaires.

List of Figures

List of Tables

Chapter 1

INTRODUCTION

1.1 General Introduction

Recently, many workers have become interested in the study of the properties of AB_2C_4 (A = Zn, Cd, Hg, Pb, Mn; B = Ga, In; C = S, Se, Te). Many of these compounds exhibit wide transparency intervals, high values of nonlinear susceptibility, natural birefrigences, optical activity, high photosensitivity, strong luminescence combined with large band gap which make them promising optoelectronic materials.

But despite the great deal of work in the study of these compounds, many

problems are still unsolved. One of these problems is the growth of big single crystals and thin films with high optical quality and controlled composition. Another problem is the origin and nature of the localized levels which are systematically present in these compounds; only some hypotheses have been formulated concerning the origin of these localized levels. On the other hand, the nature of the transitions across the band gaps and the values of these gaps are still a matter of controversy. Future applications of these compounds depend mainly on the progress in solving these problems and also in understanding how physical parameters (energy gap, refractive index,...) change with the partial isoelectronic substitution of one (or more) of the components; by properly choosing the ternary end-members, particular properties can be obtained in multinary systems.

1.2 Arrangement of the material of the thesis

This study on AB_2C_4 semiconductors is limited to materials in which A = Cd, Zn; B = Ga, In; C = S, Se, Te (except in Chapter4 where we will be dealing also with A = Pb). Emphasis will be placed on the $CdIn_2S_4$

compound; it is the most studied member of the family. But even when we will be dealing exclusively with the $CdIn_2S_4$ semiconductor (Chapter 3 and 5), we will try to relate that to the "common" properties of the whole family.

Chapter 2 is a critical review of the literature; this reveals not only the general trend observed in these compounds but also the discrepancy in the data reported by various workers. This may help in finding possible ways to study these compounds more effectively.

The method of preparation of $CdIn_2S_4$ polycrystals and single crystals (by the Bridgman-Stockbarger technique) will be given in details in Chapter 3. This method can be applied to other members of the family under conditions outlined there.

In Chapter 4, we applied for the first time the "generalized approach to the defect chemistry of the ternary compounds" developed by Groenik and Janse to the AB_2C_4 family. We show the dependence of the intrinsic defects in these compounds on the deviation from molecularity and stoichiometry due to their incongruent evaporation.

Chapter 5 deals with the optical absorption edge of $CdIn_2S_4$. A comparative analysis of the data reported for the energy gaps of this compound and the possible reasons for the discrepancy is given there. Also, in that chapter, we discuss the absorption tail below the fundamental absorption

edge and its relation with the trap distribution below the conduction band. In Chapter 6, we present some conclusions regarding the properties of $CdIn_2S_4$ in particular and AB_2C_4 family in general. Some suggestions for further studies of these compounds are also given there.

Finally, at one stage of the thesis, we were thinking to study the changes in optical parameters of AB_2C_4 compounds and their alloys with the isoelectronic substitution of one of the components. Although we could not do that experimentally, we studied from the data reported in the literature the changes in refractive index as a function of isoelectronic substitution of one element of the compound. This study has revealed a general trend in these changes not only for the ternary compounds but also for the non-metallic compounds. This may be very useful in regard to choosing specific multinary compounds for engineering purposes. This work has been submitted to Phys.Stat.Sol. Journal and is included in Appendix A.

Chapter 2

AB_2C_4 SEMICONDUCTORS : A REVIEW OF THE LITERATURE

2.1 Introduction

The present chapter deals with the results obtained in investigations of the structure, the crystal growth, the optical and photoelectric properties of the ternary nonmagnetic AB_2C_4 semiconductors in which $A = Zn, Cd$;

$B = Ga, In$ and $C = S, Se, Te$. The main attention will be concentrated on $CdIn_2S_4$ compound because it is the most studied member of the family and also because it is the main subject of this thesis.
Excellent reviews of the properties of these compounds have been published in the past few years [1,2,3].

2.2 Crystal Structure

A detailed X-ray diffraction investigation of AB_2C_4 compounds was carried out for the first time by Hahn and his colleagues [4]. They established that these compounds crystallize in lattices of two types :

- With cations only in the tetrahedral environment;
- With cations in both tetrahedral and octahedral environments.

The first type of lattice is typical of the majority of AB_2C_4 crystals. The tetrahedral structure with the space group $I\bar{4}$ (known also as Thiogallate or defect chalcopyrite) is the most frequently encountered. This structure

is the chalcopyrite structure with half of one of the cations removed [5] and these empty sites (known as stoichiometric voids) are ordered (Fig. 2.1).

Some AB_2C_4 compounds with the tetrahedral coordination of the cations appear also in two other structures [5] : the pseudocubic structure (space group $P\bar{4}2m$) and the defect stannite structure (space group $I\bar{4}2m$) (Fig. 2.2 and 2.3).

Lattices of the second type are characteristic only of AIn_2S_4. In particular, $ZnIn_2S_4$ (space group R3m) has a layered hexagonal structure based on a twelve-layer close packing of the sulfur atoms [6]. The Zinc atoms occupy only the tetrahedral voids in the lattice, whereas the Indium atoms occupy both the tetrahedral and octahedral voids (Fig. 2.4).

The layered structure seems to be an intermediate between the spinel on one hand and the tetrahedral structures on the other [26].

The second type of lattices applies also to $CdIn_2S_4$ (space group Fd3m). This compound crystallizes in the spinel structure, characterized by a cubic close packing of the anions; the Cd atoms occupy only tetrahedral voids in the lattice, whereas the In atoms occupy the octahedral voids [4] (Fig. 2.5 a). However, it has been shown later [8,9] that the most probable structure is a partly inverted spinal (Fig. 2.5b), represented by the formula

$$Cd_{1/2}In_{1/2}[Cd_{1/2}In_{3/2}]S_4$$

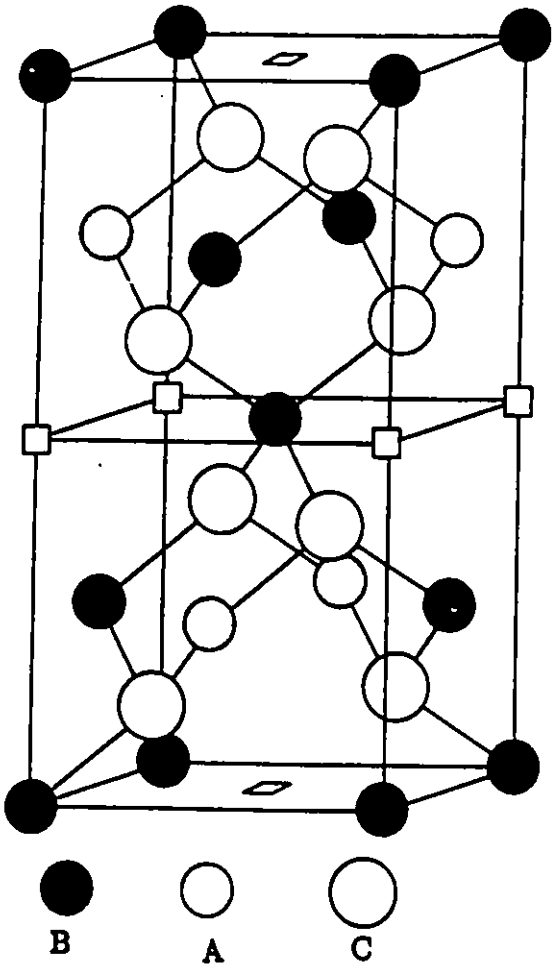

Figure 2.1: The Thiogallate Structure [5].

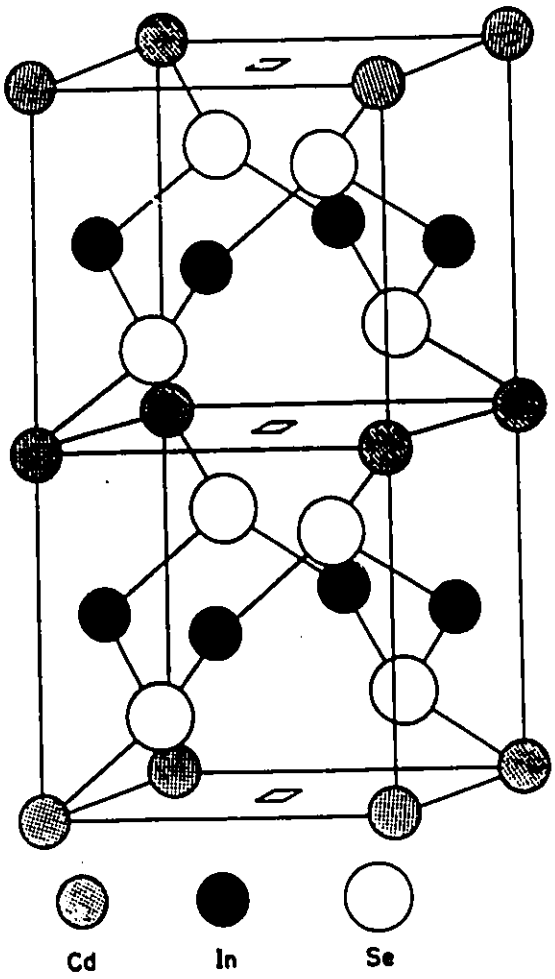

Figure 2.2: The Pseudocubic Structure [5].

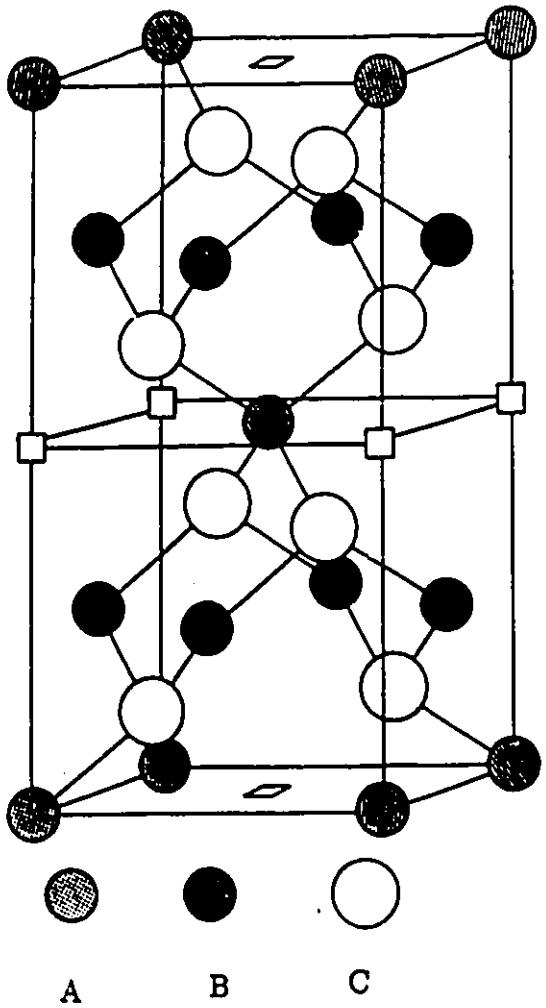

Figure 2.3: The Defect Stannite Structure [5].

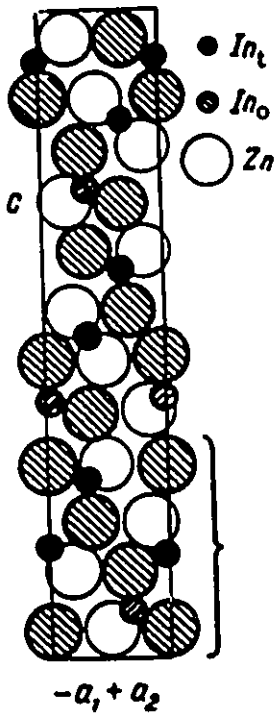

Figure 2.4: The Layered Structure [6].

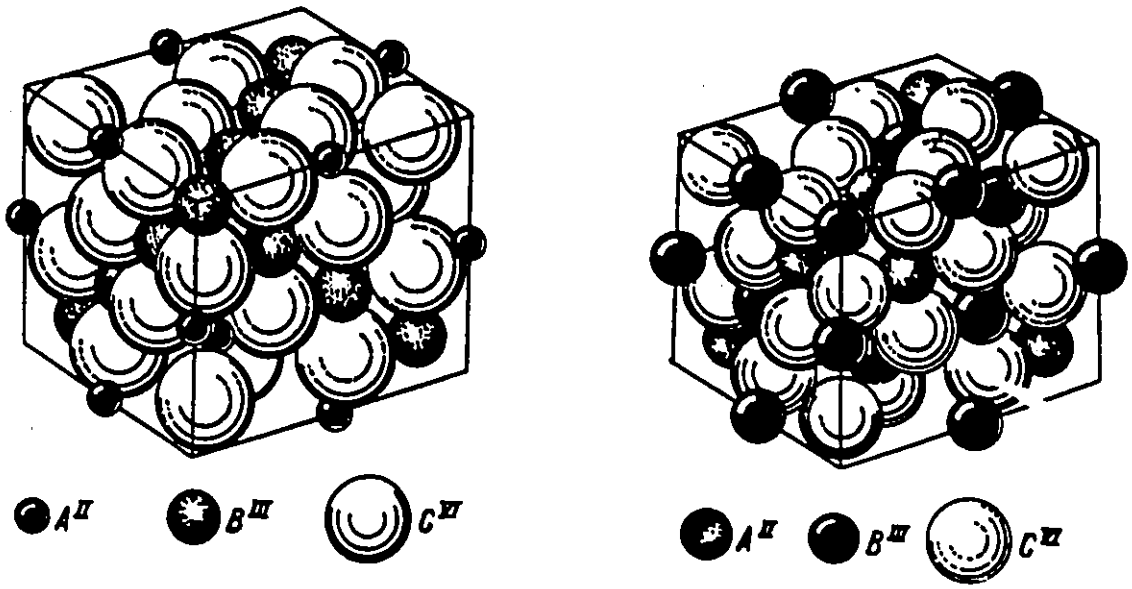

(a) (b)

Figure 2.5: The Normal (a) and The Inverted (b) Spinel Structures [6].

where the cations occupying octahedral sites are in brackets. This compound possesses an order-disorder transition at $T_c = 403K$ [8] ; for $T < T_c$, tetrahedral In and Cd atoms occupy their own sites in the elementary cell, while for $T > T_c$, Cd and In are distributed randomly on the tetrahedral sites.

Some information on the structure of the most widely encountered modifications of AB_2C_4 compounds are summarized in table 2.1. We point out that when the X-ray scattering powers of the two cations are similar (as in the case of Zn and Ga, or Cd and In), the exact structure can be difficult to determine, and several possible structures are listed for some of these compounds.

As far as we know, no definitive theories have been advanced to explain why any of these structures should be preferred, although Philpsborn [10] has discussed this question in terms of coordination numbers and polarization effects.

Crystal Family	Cations environments	Structure and space group	Compounds
AB_2C_4	Tetrahedral	Thiogallate ($I\bar{4}$)	$CdGa_2(S, Se, Te)_4$ $CdIn_2Te_4$ $ZnGa_2(S, Se, Te)_4$ $ZnIn_2(Se, Te)_4$
		Pseudocubic ($P\bar{4}2m$)	$CdIn_2Se_4$
		Defect Stannite ($I\bar{4}2m$)	$ZnGa_2(S, Se, Te)_4$
	Tetrahedral and Octahedral	Spinel (Fd3m)	$CdIn_2S_4$
		Hexagonal layered structure (R3m)	$ZnIn_2S_4$

Table 2.1: Crystal Structure of Some AB_2C_4 compounds.

2.3 Crystal Growth

Microcrystalline samples of some AB_2C_4 semiconductors have been firstly grown by Hahn et al.[4] starting from the binary compounds. Single crystals of these materials were first grown by Nitsche et al. [11] by the chemical transport technique using the iodine as the transporter. Later, Suchow et al. [12] have reported the successful growth of $CdIn_2S_4$ single crystals by the Bridgman method. Various methods are currently used to prepare these compounds [1] :

- The fusion of A, B and C components (F.C) or that of binary AC and B_2C_3 (F.B.C);
- The chemical transport reactions (C.T.R);
- The growth from the melt (G.M) (Bridgman method);
- The zone melting (Z.M);
- The growth of thin films.

Naturally, the F.C and the F.B.C produce polycrystalline samples. The C.T.R technique allows one to obtain single crystals of small dimensions (few mm^3) but this method has the disadvantage of introducing a fourth

element (used as the transport gas) in the crystal. The influence of this element on the properties of these materials is still unclear. Only the G.M and Z.M methods can produce big single crystals of high purity [13,14]. So, let us look in some details at these two techniques.

The melting character of AC-B_2C_3 quasi-binary system has been analyzed in [15]. Only $CdGa_2(S,Se)_4$ and $CdIn_2S_4$ are melted congruently. The homogeneity range of AB_2C_4 compounds at the AC-B_2C_3 quasi-binary cut is rather large ($3-7$mol%).

Because most of these compounds melt incongruently, in the zone recrystallization it is necessary to use the special method described in ([6],p.38). In view of this, one must view with suspicion the suggestion made in [16] that selenides and tellurides can be prepared by the standard zone recrystallization technique.

Although the Bridgman-Stockbarger method is potentially useful and widely used for all these compounds with melting points less than 1300 ^{0}C [14], the degree of success depends on maintaining stoichiometric composition in the melt. If one takes into consideration the tendency of ternary materials to deviate from stoichiometry then it becomes clear that a strict control of the compcsition of the samples is badly needed. The composition of the vapor over the melt is very complicated [17] and the introduction of an excess of one volatile does not really help in controlling the stoichiometry

of the crystals. It is essential to know the P-T-X phase diagrams which are not available for most of these compounds.

The works concerning the growth of thin films are not numerous yet [18,19]. We point out that these films exhibit the same tendency to deviate from stoichiometry.

In the next chapter we will discuss in details our own attempts in obtaining single crystals of $CdIn_2S_4$ by the Bridgman technique.

2.4 The Fundamental Absorption Edge

The fundamental absorption edge of AB_2C_4 has been studied extensively. Unfortunately, there exists a big discrepancy between the results obtained by different authors. This fact is likely to be due to differences in the growth conditions and consequently in the composition of crystals used by different authors [3]. The most reliable data on E_g of these compounds are listed in table 2.2. As an example, we will discuss in some details the fundamental absorption edge of $CdIn_2S_4$.

The interband transitions of this crystal have been investigated by reflec-

Compound	E_g(ev)	Type of transition
$ZnGa_2S_4$	3.18	direct
$ZnGa_2Se_4$	2.17	direct
$ZnIn_2S_4$	2.86	direct
$ZnIn_2Se_4$	1.63	indirect
$ZnIn_2Te_4$	1.52	—
$CdGa_2S_4$	3.58	direct
$CdGa_2Se_4$	2.57	direct
$CdIn_2S_4$	2.28	indirect
$CdIn_2Se_4$	1.48	indirect
$CdIn_2Te_4$	1.22	direct

Table 2.2: Energy gap (R.T.) and minimum band-band transition in some AB_2C_4 compounds [1,3].

tivity, absorption, photoconductivity, photoluminescence and photovoltaic effect [3,20]. It has been established that $CdIn_2S_4$ is an indirect semiconductor, but the agreement among the experimental data is very poor. Thus, at room temperature, values of the direct gap E_g^d ranging from 2.10 to 2.62 ev, and from 2.00 to 2.28 ev for the indirect gap E_g^i are reported in the literature. Obviously, various authors have prepared and investigated samples with different composition [21]. Calculations of the energy band structure of this compound are reported. According to [22], $E_g^i = 2.35$ ev and $E_g^d = 2.40$ ev.

Before we leave this section, we should point out that absorption tails have been found in the energy range E < E_g. This behaviour will be considered later.

2.5 The Localized Levels

Despite the great deal of work in the study of the properties of AB_2C_4 semiconductors, a systematic study of the origin and characteristics of the localized levels in these crystals is still lacking. However, a detailed analysis of the papers published regarding the properties of these compounds can lead to a reasonable picture on the localized levels.

2.5.1 Effects of The Crystal Growth Conditions

All the compounds, even if grown with different techniques, display n-type conductivity. The intentional crystal doping with first group or fifth group impurities does not change the sign of the majority carriers [2]. A strong dependence of the sample resistivity on the chalcogen concentration during the growth is reported in the literature. For instance, the resistivity of $CdIn_2S_4$ is maximum in samples grown with excess of Sulfur [2]. This indicates that the crystals tend to grow with chalcogen vacancies which produce relatively deep donor levels (in $CdIn_2S_4$, a donor center located at 0.5 ev below the conduction band is associated with sulfur vacancies [23]).

2.5.2 Shallow Donors

In the investigation of the fundamental absorption edge of AB_2C_4 crystals, a strong absorption of light has been found in a wide range of photon energies such that E<E_g. It was found also that the absorption coefficient α depends exponentially on the photon energy [2,3]. These absorption tails are attributed to the absorption by a quasicontinuous distribution of traps just below the conduction band. It is believed that the concentration of these traps N(E) decreases with depth in the band gap in accordance with

the law,

$N(E)=N_0\exp(-\alpha E)$

In the case of $CdIn_2S_4$, α is about 39 ev^{-1} [2] and is not strongly dependent on the temperature according to [24].

The presence of these shallow donors is supported by the photocurrent, thermoluminescence and thermally stimulated conductivity measurements ([3] and references therein).

Whether these traps are really made of continuous levels or of discrete levels is not totally clear. However, in the case of $CdIn_2S_4$, a recent study [25] suggests that these traps are mainly made of discrete levels. This view is supported by several factors. Among these is the fact that the thermally stimulated conductivity depends strongly on the wavelength of the exciting light. If traps were made from continuous levels interacting with each other, then this effect could not be observed because electrons tend to be distributed in thermal equilibrium state even though the exciting energy is too low to fill the deep levels.

2.5.3 Shallow Acceptors

Because the AB_2C_4 compounds are very compensated, shallow acceptors with high density must be present in these crystals. Indeed, a high density of shallow acceptors (N_A=$10^{18}cm^{-3}$) has been reported for $CdIn_2S_4$ [26]. One explanation of this high density of acceptors is the possibility of In-Cd exchange connected with the order-disorder transition.

2.5.4 Deep Levels

Many different deep levels have been evidenced in AB_2C_4 single crystals [2]. We point out that in many compounds, a deep double charged acceptor has been found. The origin of this acceptor center is still unclear.

A common picture of localized levels in AB_2C_4 semiconductors has been proposed by Grilli et al. [2], and the energy-level scheme of this model is shown in Fig. 2.6.

Let us now analyse the photoluminescence and the photoconductivity of $CdIn_2S_4$ single crystals and relate them to the localized levels in this crystal.

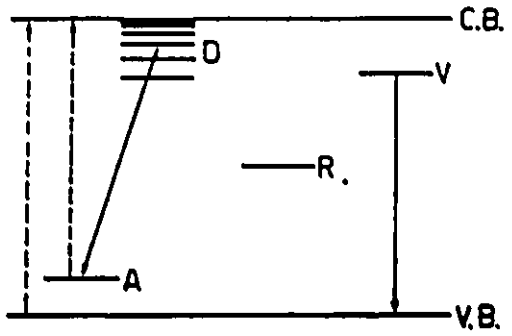

Figure 2.6: Energy-level diagram of AB_2C_4 Compounds [2].

2.6 Photoconductivity And Photoluminescence of $CdIn_2S_4$ Single Crystals

Studies of the photoconductivity spectra of $CdIn_2S_4$ single crystals are reported in ([3] and Ref. therein). More detailed information is given in [27] where a study of as-grown crystals and the influence of nonstoichiometry as well as of annealing and argon ion implantation revealed four photoconductivity (Phc) peaks at 2.5 ev; 2.1 ev; 1.8 ev and 1.4 ev (at T=80K). The peak at 2.5 ev is believed to be caused by the direct interband transition. The Phc peak at 2.1 ev may be connected with the ionization of the accep-

tor center Cd_{In}. The peak at 1.4 ev appears to be caused by In_{Cd} defects. The origin of the Phe peak at 1.8 ev is unclear.

The photoluminescence (Phl) spectrum of $CdIn_2S_4$ consists of a wide band with a maximum in the region $1.4 - 1.9$ ev. This band is complex and it consists of four simple bands located at 1.77 ; 1.65 ; 1.45 and 1.30 ev (at T=80 K) [27]. From the study of the influence of nonstoichiometry, the annealing and ion implantation [27], it was concluded that the Phl peak at 1.3 ev is associated with In_{Cd} defects. The one at 1.77 ev is bound with the Cd_{In} centers. The bands at 1.45 and 1.65 ev are related with V_{Cd} and $(V_{Cd}I_S)$ complexes respectively.

From an analysis of the electron lifetime and the rate of trapping of electrons, Takizawa et al. [25] claimed that excited electrons recombine with holes only through the conduction band. This is in contradiction with the model of recombination processes reported in [28] where some luminescence bands are attributed to electron transition from the trap distribution below the conduction band to an acceptor level.

In general, an analysis of the published data on the photoluminescence of AB_2C_4 compounds makes it possible to identify the following common features [2,3] :

- The Photoluminescence of these crystals depends on the composition and the method of preparation;
- The emission spectrum is generally composed of a wide gaussian band, whose energy is of the order of one half of the energy gap;
- the interband radiative recombination is exhibited only by $CdGa_2(S, Se)_4$ crystals;
- AB_2C_4 contain not only luminescence centers, but also nonradiative recombination centers, as confirmed by the thermal quenching of the photoluminescence.

2.7 Other Properties of $CdIn_2S_4$

Non-linear conduction in $CdIn_2S_4$ single crystals i.e., low frequency oscillations, switching and memory effect, have been observed by several workers ([29] and Ref. therein). Saturated photoconductivity has been reported in [26]. Studies have been made of n-$CdIn_2S_4$/p-$CuInSe_2$ and n-$CdIn_2S_4$/p-$HgCr_2Se_4$ heterojunctions ([3] and Ref. therein). Also, electroluminescence and optical gain were reported in [30] and [31] respectively. Finally, the photoacoustic spectra of this crystal was measured by Kouichi et al.

[32].

2.8 Ternary Semiconductor Alloys

In order to gain further insight into the influence of the lattice disorder on the localized levels in AB_2C_4, many workers have undertaken an analysis of the pseudoternary alloys with partial substitution of one of the cations or of the anion ([33] and Ref. therein). Also, by properly selecting the ternary end-members, particular properties can be obtained in the quaternary system, because these properties (especially the energy gap and the refractive index [34,35]) change in a predictive way with the isoelectronic substitution (see Appendix A).

One significant conclusion [36] is that the alloy process does not modify in a significant way the density of the localized levels in comparison with the ternary compounds. The main characteristics of the recombination process in the quaternary systems recall effects that are typical of AB_2C_4; the shape of the emission band, the dependence of the emission band halfwidth on the temperature, and the presence of shallow acceptor levels [37]. This confirms that the photoelectronic properties of AB_2C_4 compounds follow a common trend that can be associated with the high density of intrinsic

defects connected with the complexity of their structure.

Chapter 3

CRYSTAL GROWTH OF

$CdIn_2S_4$

3.1 Introduction

A number of techniques have been described in the literature for the growth of AB_2C_4 including melt growth [12,23,14] and growth by vapour transport [11].

We investigate the growth of $CdIn_2S_4$ single crystals by the Bridgman-Stockbarger method in order to develop an insight into the crystal growth

which can be applied to the members of this group.

The vertical Bridgman (Stockbarger) method of melt growth of crystals has found a fairly wide application to metals, oxides, ceramics, fluorides and semiconductors [38]. The book by Brice [39] discusses this method in detail.

3.2 Description of The Bridgman-Stockbarger Technique

The Bridgman-Stockbarger technique produces nucleation on a single solid-liquid interface by carrying the crystallization in a temperature gradient. The material to be crystallized is in a crucible of suitable geometry, which is lowered through the temperature gradient or the heater is raised along the crucible. In some cases the crucible is held stationary in the furnace and the furnace is then cooled slowly. In this case an isotherm normal to the axis of the crucible is caused to move through the crucible slowly enough that the melt interface follows it.

The Bridgman growth requires :

- A crucible of suitable geometry,
- A suitable furnace capable of producing the desired gradient,
- Temperature measuring and control equipment and in some cases equipment for programming temperature or equipment for lowering the crucible.

The crucible is made such that the freezing of the melt starts at a point or constriction. As the solidification proceeds a faster growing seed usually outstrips the others and a single crystal is produced. To ensure that only one crystal is formed, a constriction may be introduced into the tube such that the nucleation is initiated in the tip while the remaining material is above the melting point [39] (Fig. 3.1). The melt must be unreactive with the crucible material at the growth temperature . Also, the crystal must not stick to the crucible because such behaviour has a deterious effect on the crystal surface and its homogeneity. Silica is the most useful crucible as the charge can be completely enclosed and sealed off so that no contamination or loss of vapour is possible. Unfortunately, several molten materials show a pronounced tendency to stick to silica. This is probably due to traces of oxides formed by reaction with the silica or present in the starting materials. Some sticking may also be due to the metal keying into pores in the silica.

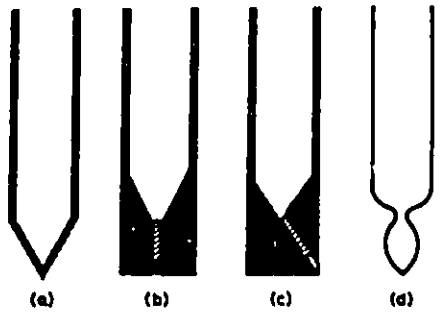

Figure 3.1: Crucibles used for the Bridgman method.

The furnace should consist of two or three regions with a minimum of thermal coupling between them. The regions should be capable of independent control and a thermal barrier should separate at least two of them. Often, a metallic sheet (Pt) whose size just permits the passage of the crucible is used for that.

The lowering rate depends on the temperature gradient at the interface. The steeper the gradient, the faster the rate which can be allowed. In particular, the lowering rate should be slow enough to permit all the heat of crystallization to be conducted away downwards through the crystal.

The solid-liqu' ' interface is then maintained planar and horizontal. If the lowering rate is too rapid, cooling may occur from the sides producing spurious crystal growth and a polycrystalline ingot.

For crystal perfection, thermal and mechanical fluctuations must be avoided. Such fluctuations cause irregular growth and the inclusion of imperfections in the crystal.

In the next sections, a description of the method used to grow single crystal of $CdIn_2S_4$ will be given.

3.3 Description of The Apparatus

3.3.1 The Vertical Furnace

This HOME-MADE FURNACE (Fig. 3.2) consists of three regions. This configuration (with three regions) has the advantage of two isothermal regions with a gradient between them which permits annealing the crystal after growth without introducing a large thermal strains. A metallic sheet separates the 1st and 2nd regions which tends to minimize the thermal coupling between them. The regions are independently controlled

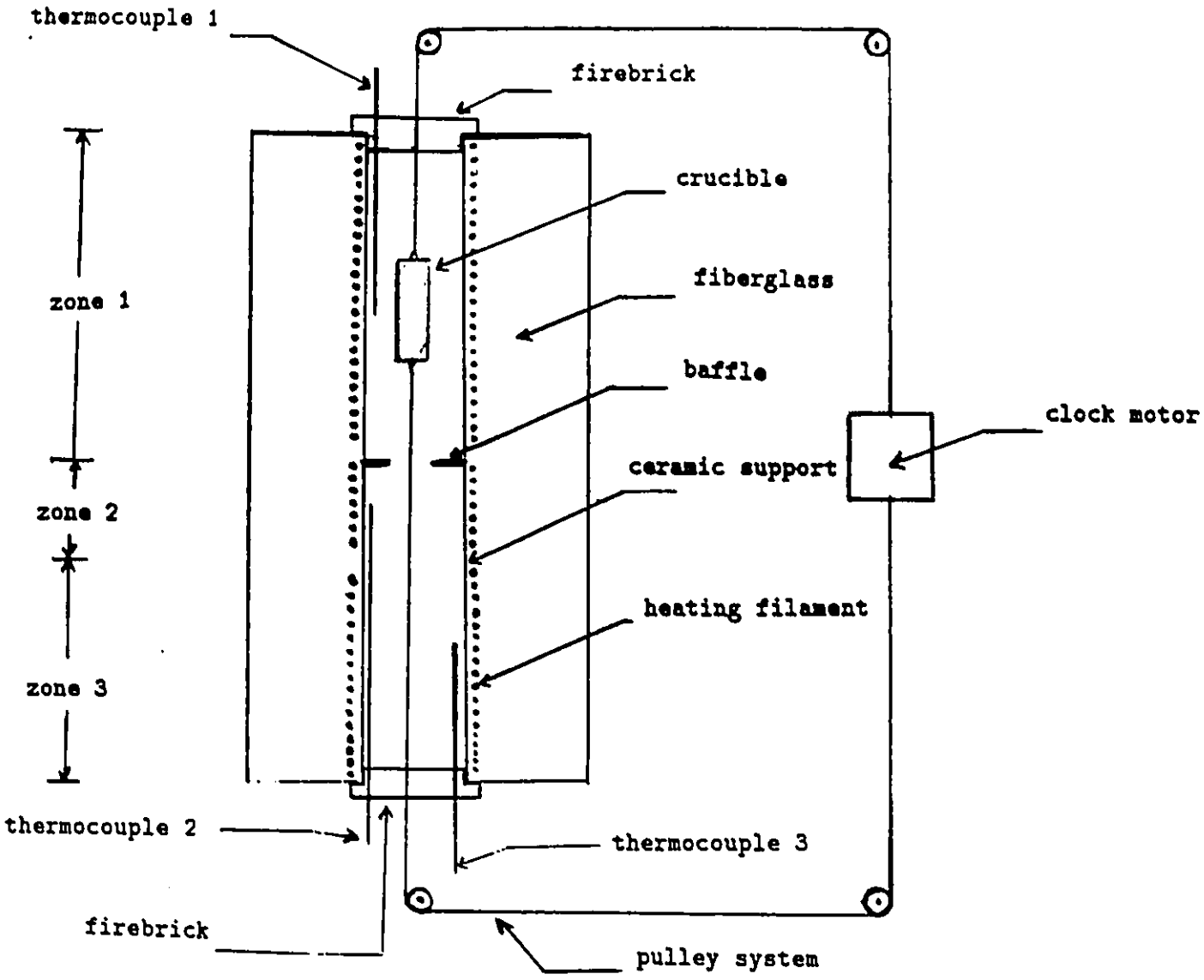

Figure 3.2: Detail of the Vertical Furnace arrangement.

by an ANA-LOCK CONTROLLER (THERMCO PRODUCTS CORPORATION, MODEL 321) which compares recorded temperatures with the requested values and outputs an analog 0-5 v signal via an amplification-differentiation-integration servo-loop. This error signal controls the duty cycle of a pulse-length modulated square wave synchronized with the AC line which in turn opens and closes a solid state relay providing power to the heating elements of the furnace. This servo-control system provides an accurate control of the melt temperature. The thermal fluctuations are almost eliminated ($< \pm 0.05\%$).

Three type "R" thermocouples (100% Platinium(+), 87% Platinium(-)) have been used to measure the temperatures inside the regions.

The resistances are metal wires (nichrome or kanthal) wound on a cylindrical support made of ceramics. The coils are fixed to the support by covering them with the Al_2O_3 paste. The whole is surrounded by a suitable thickness of fiberglass insulating material. Heat loss at the ends of the furnace is compensated by an increase in the density of turns of the heating filament.

The method used to lower the crucible inside the furnace is to attach it to a motion controller (clock motor) through a suitable pulley system (Fig. 3.2). Transmission of the motion to the crucible through a rigid support,

such as a rod attached to the crucible, was also used. Great care was taken to avoid mechanical fluctuations.

This furnace has been used to grow $CdIn_2S_4$ single crystals by the Bridgman method.

3.3.2 The Horizontal Furnace

This LINDBERG 3-ZONE TUBE FURNACE (Fig. 3.3) has been designed with ample reserve power in the ends to compensate for inherent heat losses out of the ends of the furnace. The greatest furnace temperature uniformity exists in the center zone, over a length that reaches almost to the ends of the center zone heating unit. This length will change depending on how one balances the end zones. The furnace has been designed to provide a rapid heat up rate, to eliminate the need of continuous operation at maximum temperature.

The furnace contains three PLATINE2 thermocouples. In addition, it is necessary to use two separate monitoring thermocouples to read the temperature differences between the center zone and the end zones.

An EUROTHERM MODEL 211 (a seven segment PROGRAMMER/CONTROLLER)

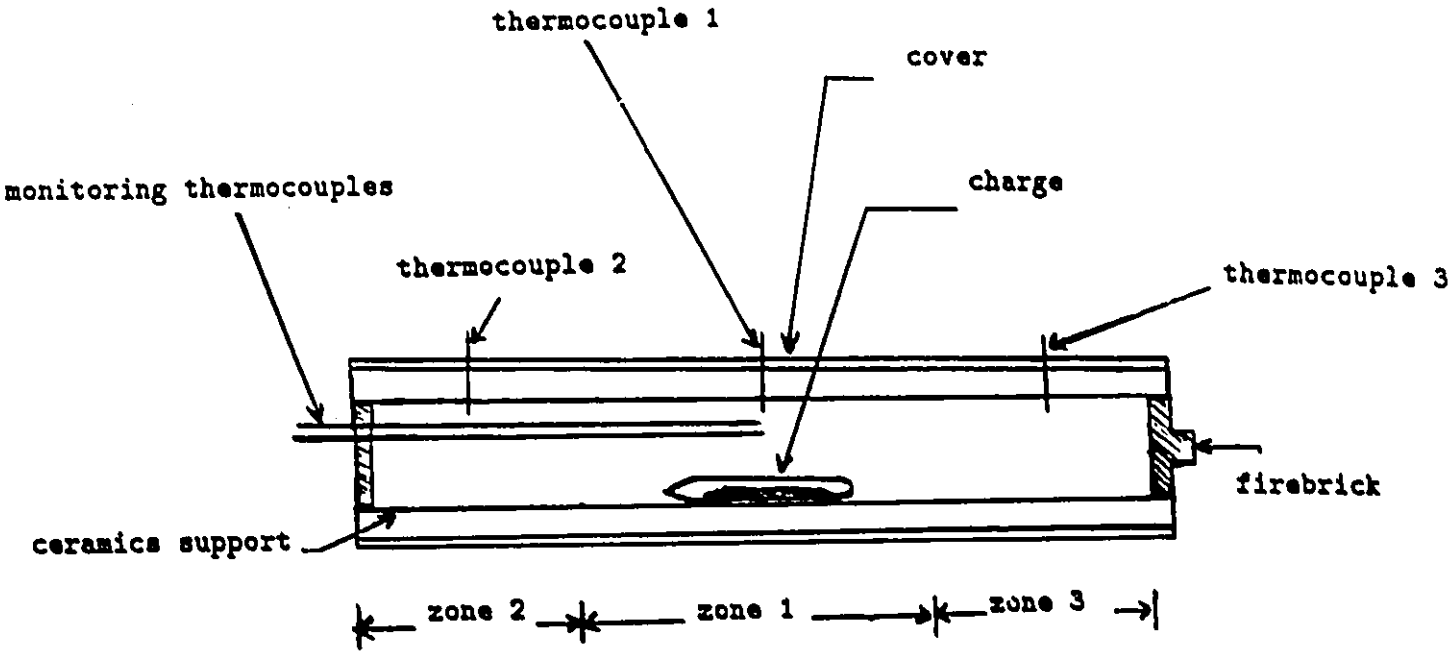

Figure 3.3: The Horizontal Furnace.

was used as a control system between the furnace and the power line. Each segment may be set to either a ramping or a hold segment or may optionally be removed by setting the segment as a hold segment with zero time.

Features of this programmer are :

- Input of level and time in engineering units,
- Interrogation of the program at any time,
- Modification of the program during operation,
- Security key to prevent modification by unauthorized personnel,
- Linearization of output to suit most common thermocouples,
- Data retention during power failure,
- Display of the setpoint or the time remaining in the segment.

Because of its temperature uniformity which provides a very homogeneous melt, this furnace has been used to prepare $CdIn_2S_4$ polycrystals.

3.3.3 Ampoules Preparation

All experiments were carried out in silica tubes. In preliminary experiments it was observed that a reaction occurred between the compound and the quartz walls of the ampoule to form silicates of the metals present. This behavior unknown in the literature until recently [40] influences the composition of the crystal. This reaction has also a deterious effect on the surface of the crystal.

This reaction could be reduced and almost eliminated by a suitable quartz preparation technique. A similar procedure was used by Haupt and Hess in their work with $CuInSe_2$ [41].

The ampoules were systematically :

- Flame polished from one end to the other,
- Degreased with Acetone, to remove traces of organic compounds from the surface of the quartz (rectified Ethyl Alcohol may be used),
- Etched in hydrofluoric acid (HF40%) for $3-5$ minutes in order to clean the internal surface and remove small projections which might act as spontaneous crystallization centers; this should be followed by

washing in distilled water and dried in order to remove any traces of the acid.

- Finally, heated under vacuum at about 1000 ^{0}C for several hours, in part to remove traces of water.

3.4 Growth Procedure

3.4.1 Growth of $CdIn_2S_4$ Polycrystals

During the course of the investigation, crystal growth was pursued by two different techniques :

- Direct reaction of the constituent elements in a sealed, evacuated ampoule :
  $Cd + 2In + 4S \rightarrow CdIn_2S_4$
- preparation of the crystal from the binary compounds :
  $CdS + In_2S_3 \rightarrow CdIn_2S_4$

In the first technique, stoichiometric quantities of the elements are weighed and sealed under vacuum (better than 10^{-5}Torr) in a quartz tube which had

been cleaned as described earlier. The tubes are cylindrical with a point on the lower end; typical dimensions are $15cm \times 10mm$. Total contents are usually $3-6$g. The materials are initially reacted by heating in the furnace. Great care was taken in this process to heat very slowly to avoid explosive reactions, particularly between In and S. In spite of this, excessive pressure build up always causes the tube to explode.

Endo et al. [23] have reported such growth : the tube was heated to about 500 ^{0}C at a rate of 2 degrees per hour, held at this temperature for about one week then heated to about 1200 ^{0}C at the same rate as before and maintained for one week. The tube was then cooled down to room temperature at the same rate as that for heating (the whole process takes about 2 months!!). This procedure is not possible with the furnaces we have in hand.

In the second technique, polycrystals of $CdIn_2S_4$ were synthesized by firing stoichiometric mixtures of binary chalcogenides CdS (99.999%) and In_2S_3(99.999%) with or without an excess of sulphur in quartz tubes which had been cleaned as described earlier and evacuated to about 10^{-5}Torr. The fine powders of the binary compounds were supplied by Johnson Matthey Chemical Limited.

The quartz tubes were set horizontally in the horizontal furnace whose heat-

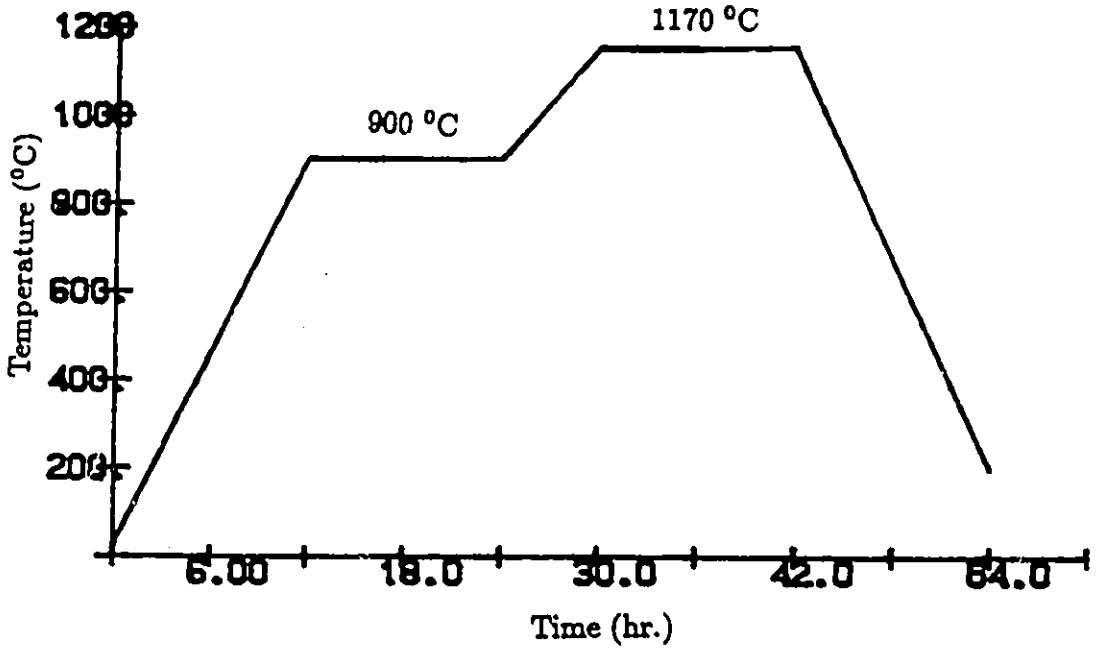

Figure 3.4: Heat treatment program used to grow $CdIn_2S_4$ polycrystals.

ing and cooling were controlled according to a fixed timetable (Fig. 3.4).

After the freezing process, the samples were allowed to cool in the furnace, ground and heat treated for a second period to ensure complete homogenation.

During this synthesis, a slight loss of S was inevitable. Small amounts of S were found on the walls of the quartz tube. No reaction between the crystal

and the quartz ampoule was observed.

When growing the crystals it is usual to hold the melt temperature initially above the melting point to ensure complete melting of the charge. However, caution must be exercised since the material tends to decompose at temperatures greatly in excess of the melting point, causing explosion by failure of the quartz tube.

Finely Powdered mass of the ingot was analyzed by Debye-Scherrer X-ray diffraction at room temperature with Cu $K\alpha$ radiation and Ni filter; in agreement with Suchow's results [12] a complete correspondence with $CdIn_2S_4$ X-ray spectrum was observed.

3.4.2 Bridgman Growth of $CdIn_2S_4$ Single Crystals

The Bridgman-Stockbarger had been successfully used in previous occasions to grow $CdIn_2S_4$ single crystals [12,14,23].

In our case, the Bridgman ampoules had an inner diameter of 10mm and a length of $12 - 15cm$ and were prepared as described earlier. The tubes were tapered at the bottom to allow proper nucleation (Fig. 3.1d).

As starting materials, polycrystalline $CdIn_2S_4$ (prepared by firing the binary compounds as described in the previous section) were used. The ampoules were evacuated to 10^{-6} Torr, and were then sealed and positioned in the hot zone of the vertical furnace whose temperature was set at 1170 ^{0}C in order to establish an optimum thermal profile. As stated previously, caution must be exercised in setting the high temperature of the furnace; the temperature used is above the melting point of the ternary compound in order to have homogeneous melt but still prevent thermal dissociation of the molten ternary. The temperature distribution of the furnace and the initial setting position of the ampoules are shown in Fig. 3.5. Prior to crystal growth, the melt was heated at least 12 hr in the hot zone to promote homogeneous solidification.

We realized crystal growth from the melt in the following way:
The furnace was controlled at constant temperature and the ampoule was lowered by $0.5 - 1.0$ cm/hr through the temperature gradient which was usually $25 - 35$ ^{0}C/cm at the melting (freezing) point of the material. At the melting point (1100 ^{0}C) quartz becomes plastic and the vapour pressure of $CdIn_2S_4$ in excess of one atmosphere expands the sealed quartz tube. This expansion typically limits the growth period to 48 – 60hr.

After the freezing process, the furnace was cooled down slowly to prevent

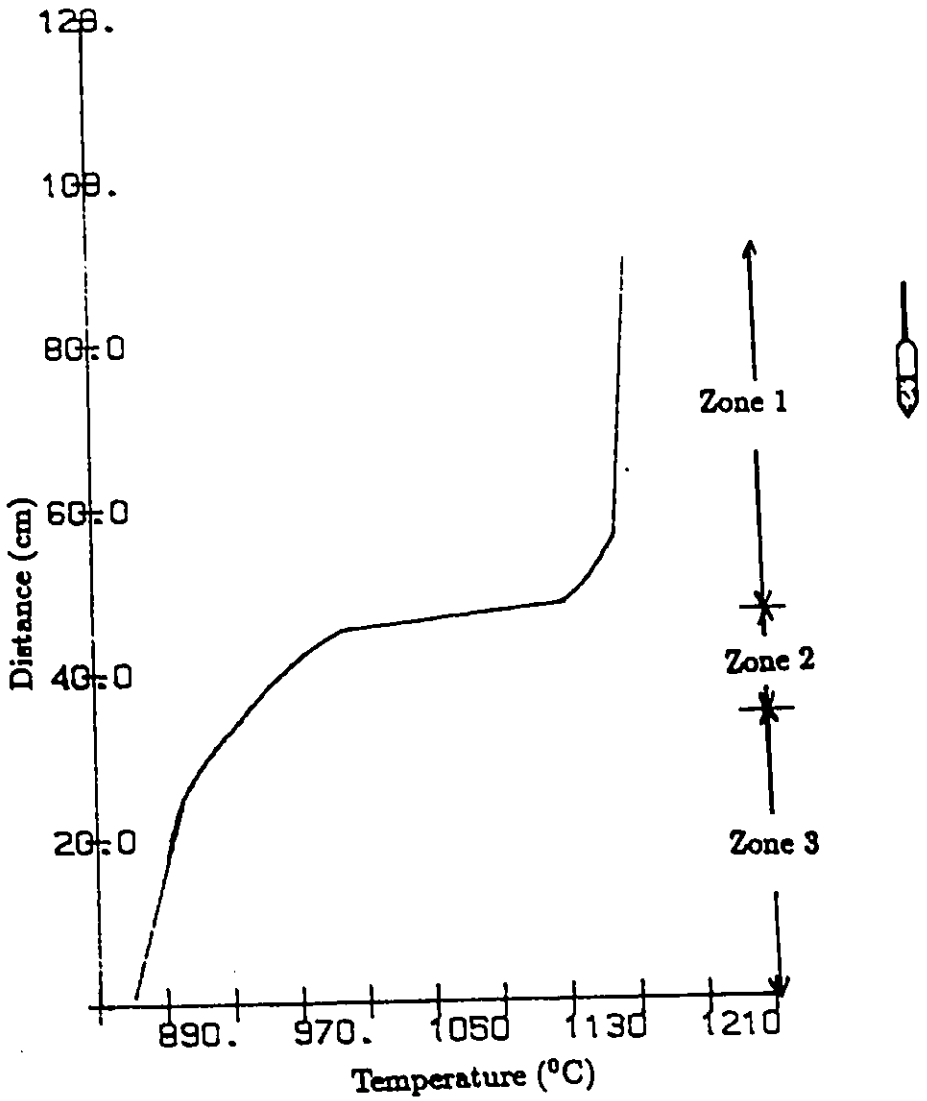

Figure 3.5: Temperature distribution of the vertical furnace and initial setting position of the ampoule.

the ampoule cracking. Then the tube was removed. The crystal was obtained after breaking the ampoule. No reaction with the quartz ampoule was observed. Samples of 1cm diameter and $4-5$cm long have been grown in this way. Laue back-reflection revealed single crystals.

A cross-section of a typical crystal is shown in Fig. 3.6. The capillary region and bottom fifth of the boule is sometimes polycrystalline and contains internal voids aligned along the growth axis. As growth continues, one of the grains eventually predominates and a large section of uncracked single crystal material is produced. At the top of the boule, we find cellular growth indicating phase separation by partitioning at the interface.

3.4.3 The Sulphur Pressure effect on Crystal Growth

The sulphur pressure dependence crystallization was examined by adding an excess of sulphur during the polycrystal preparation (about $2-5$at.%). The resulting ingots and single crystals showed obvious sulphur-pressure dependence and their outside appearances are as follows. In case of low sulphur-pressure, the ingots were porous and fragile. As the sulphur pressure increased, the ingots became harder and single crystals sizes became larger with residual sulphur on the top of the crystal. The color changed

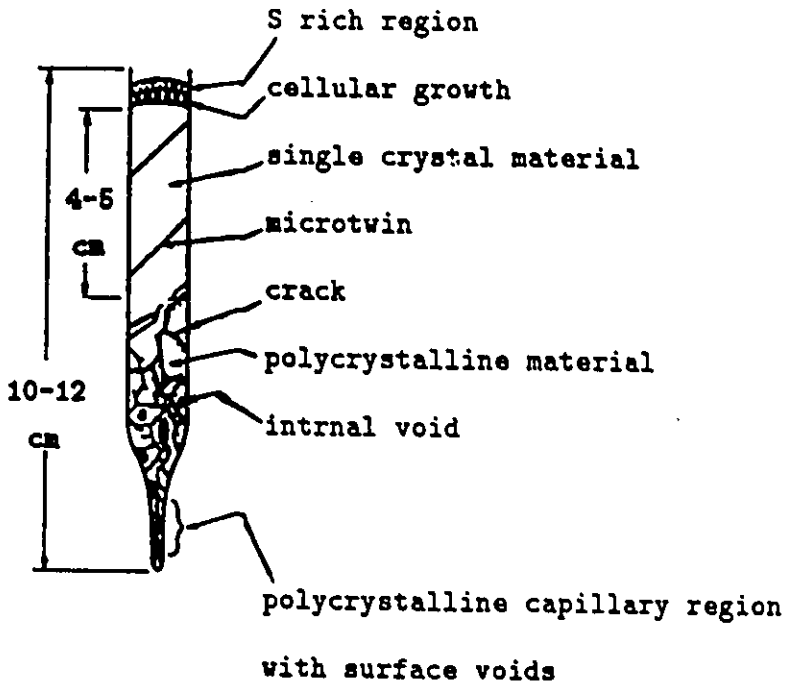

Figure 3.6: Cross-section of a typical $CdIn_2S_4$ boule.

from dark-red to red with increasing sulphur-pressure.

In conclusion, the method presented herein is believed to be applicable to all ternary chalcogenides with reasonable melting points which have no solid-solid phase transitions between room temperature and their melting points.

Chapter 4

INTRINSIC DEFECTS IN AB_2C_4: a Thermodynamic Approach

4.1 Introduction

It is a well-known experimental fact that the electrical and optical properties of AB_2C_4 semiconductors are largely influenced by growth conditions and annealing procedures from which it has been concluded that intrinsic

doping effects play an important role.

Although numerous experimental data regarding the influence of growth and annealing conditions on the properties of these compounds has been published in the literature the identification of the nature of the intrinsic defects is still an open question.

In this chapter the properties of several undoped melt grown AB_2C_4 crystals are analyzed in terms of the expected deviation from stoichiometry and molecularity due to the incongruent evaporation of most of these ternary semiconductors.

4.2 Defect Chemistry In Relation To The Crystal Composition

A ternary crystal $A_aB_bC_c$ is made up of the cations $A^{\alpha+}$, $B^{\beta+}$ and the anion $C^{\gamma-}$ and we assume that$\beta \geq \alpha$.

The following defects can be present in this crystal (using Kroger-Vink notation [42]):

$A_i^{(\alpha-j)\cdot}$	$j = 0, 1, ...\alpha$	A atom on interstitial

$B_i^{(\beta-k)\cdot}$	$k = 0, 1, ...\beta$	B atom on interstitial
$C_i^{(\gamma-l)\mid}$	$l = 0, 1, ...\gamma$	C atom on interstitial
$V_A^{(\alpha-j)\mid}$	$j = 0, 1, ...\alpha$	vacancy on A site
$V_B^{(\beta-k)\mid}$	$k = 0, 1, ...\beta$	vacancy on B site
$V_C^{(\gamma-l)\cdot}$	$l = 0, 1, ...\gamma$	vacancy on C site
$A_B^{(\beta-\alpha-m)\mid}$	$m = 0, 1, ...\beta - \alpha$	A atom on B site
$B_A^{(\beta-\alpha-n)\cdot}$	$n = 0, 1, ...\beta - \alpha$	B atom on A site
$e^{\mid}$		electron in the conduction band
$h^{\cdot}$		hole in the valence band

In this notation, the superscript ($^{\mid}$) is used to denote an electron localized at the defect whereas the superscript ($^{\cdot}$) is used to denote a hole localized at the defect.

Defects such as an anion on a cation site were omitted because these are unlikely owing to the very high formation energy with respect to other defects [43].

Concerning the electrical activity (donor or acceptor) of the intrinsic defects considered here; in both the ionic and covalent bonding models, anion interstitials (C_i), cation vacancies (V_A, V_B), and A atoms on B sites (A_B) are acceptors whereas cation interstitials (A_i, B_i) and B atoms on A sites (B_A) are donors. The only difference between the two models concerns the

anion vacancies (V_C) which are donors in the ionic model and acceptors in the covalent model [44].

Now, if the influence of nonstoichiometry on the formation of intrinsic defects in AB_2C_4 crystals is considered, it must be taken into account that any ternary compound with this chemical composition deviating from the ideal atomic stoichiometry (1 : 2 : 4) but located at the quasi-binary cut $AC - B_2C_3$ is stoichiometric in the sense of valence stoichiometry because the number of cation valence electrons is exactly right to satisfy the anions requirements. Thus, intrinsic defects will only be formed in such cases where besides a deviation from the ideal atomic stoichiometry there is also a deviation from valence stoichiometry. Recently, this problem has been studied in details in a general approach to the defect chemistry of ternary compounds [43]. The following discussion is based on that approach.

We consider the ternary crystal $A_aB_bC_c$ (in our case $a : b : c = 1 : 2 : 4$) to be made up of $LA_pC_q + MB_rC_s + NC_2$. We choose L, M, N, p, q, r, and s in such a way that this equation corresponds to the vaporization reaction of the compound. The reason for this choice will be clear later. The total concentrations of A, B and C in the crystal are :

$$[A]_{tot} = L.p = [A_A^x] + \sum_{j=0}^{\alpha}[A_i^{(\alpha-j).}] + \sum_{m=0}^{\beta-\alpha}[A_B^{(\beta-\alpha-m)|}] \tag{4.1}$$

$$[B]_{tot} = M.r = [B_B^x] + \sum_{k=0}^{\beta}[B_i^{(\beta-k).}] + \sum_{n=0}^{\beta-\alpha}[B_A^{(\beta-\alpha-n).}] \tag{4.2}$$

$$[C]_{tot} = L.q + M.s + 2N = [C_C^x] + \sum_{l=0}^{\gamma}[C_i^{(\gamma-l)|}] \tag{4.3}$$

A_A^x, B_B^x, and C_C^x denote A, B, and C atoms on their normal sites.

The composition of the crystal is known if the ratios $[A]_{tot}/[B]_{tot}$ and $[C]_{tot}/[A]_{tot}$ (or $[C]_{tot}/[B]_{tot}$) are known. For a crystal with an ideal composition these ratios are :

$$\frac{[A]_{tot}}{[B]_{tot}} = \frac{L.p}{M.r} = \frac{a}{b} \tag{4.4}$$

$$\frac{[C]_{tot}}{[A]_{tot}} = \frac{L.q + M.s + 2N}{L.p} = \frac{c}{a} \tag{4.5}$$

The deviation from the ideal composition can be described by two parameters δx and δy, defined in terms of ratios $[A]_{tot}/[B]_{tot}$ and $[C]_{tot}/[A]_{tot}$:

$$\delta x = \frac{r}{p}\left(\frac{[A]_{tot}}{[B]_{tot}} - \frac{a}{b}\right) = \frac{L}{M} - \frac{r.a}{p.b} \tag{4.6}$$

$$\delta y = \frac{\gamma[C]_{tot}}{(\alpha[A]_{tot} + \beta[B]_{tot})} - 1 \tag{4.7}$$

δx determines the deviation from molecularity, δy the deviation from stoichiometry. An excess A_pC_q gives $\delta x > 0$, an excess B_rC_s gives $\delta x < 0$. δy is

the parameter which determines, at a fixed δx, whether there is an excess C_2 (δy> 0) or a deficiency C_2 (δy< 0). When δx=δy= 0, the crystal has the ideal composition.

Now, if we use the approximation that the concentrations of two defects of opposite sign are much higher than the concentrations of all other defects [45], it has been shown in [43] that a given majority defect pair can only exist in the crystal if certain conditions with regard to δx and δy are fulfilled. A complete survey of the conditions for all majority defect pairs is given in table 4 of [43].

Recently, Neuman [46,47] has applied this approach to the ABC_2 chalcopyrites. The interesting point is that the quantities δx and δy can be derived directly from the analysis of the partial vapour pressure data of the ternary compound under consideration at the melting point or slightly higher temperatures. Although the vapour pressure data reported for ABC_2 crystals are all related to temperatures below the melting point, it has been shown [47] that an extrapolation of this data to high temperatures leads to correct prediction of the nonstoichiometry in all ABC_2 chalcopyrites. We will assume that this is true also for the AB_2C_4 semiconductors.

Let us now consider the conclusions which can be made on the basis of the partial pressure data. Obviously :

$P(A_pC_q) > P(B_rC_s)$ means a deficiency A_pC_q in the solid

phase and corresponds to $\delta x < 0$.

$P(A_pC_q) < P(B_rC_s)$ means an excess A_pC_q in the solid phase and corresponds to $\delta x > 0$.

similarly,

$(p.\alpha\text{-}q.\gamma)P(A_pC_q) + (r.\beta\text{-}s.\gamma)P(B_rC_s) > 2\gamma P(C_2)$ corresponds to $\delta y < 0$

$(p.\alpha\text{-}q.\gamma)P(A_pC_q) + (r.\beta\text{-}s.\gamma)P(B_rC_s) < 2\gamma P(C_2)$ corresponds to $\delta y > 0$

4.3 Nonstoichiometry And Intrinsic Defects In As-grown AB_2C_4 Crystals

If an AB_2C_4 growth experiment is started with a material having the ideal composition then in the resulting as-grown crystal a deviation from this ideal composition is expected because of the incongruent thermal evaporation of most of these compounds [17]. As stated earlier, because the vapour pressure data reported in ([17] and Ref. therein) are all related to temperature below the melting temperature we will assume that an extrapolation

of this data to higher temperatures leads to a correct prediction of the non-stoichiometry of these compounds. Such an assumption has been confirmed for the ABC_2 compounds [47].

The vaporization of the ternary compounds AB_2S_4 has been studied extensively [17]. For the ternary compounds AB_2Se_4, only the vaporization of $CdIn_2Se_4$ has been reported [48]. No vaporization study has been reported for the compounds containing Te.

$CdIn_2S_4$

This compound was studied in the temperature range from 1020 to 1176 K [49]. The vaporization reaction is :

$$CdIn_2S_4(s) \rightarrow In_2S_3(s) + Cd(g) + 1/2S_2(g) \qquad (4.8)$$

The vapour pressure of $In_2S_3(s)$ is negligible because the vapour of $CdS(ss)$ (ss signifies solid solution in $In_2S_3(s)$) is 100 times that of $In_2S_3(s)$. At higher temperatures the vapour pressure of $S_2(g)$ from reaction (4.8) suppresses the vaporization of $In_2S_3(s)$. Thus the deviation from molecularity is characterized by $\delta x < 0$ and the deviation from stoichiometry by $\delta y < 0$.

$CdGa_2S_4$

The chemistry and thermodynamics of vaporization of $CdGa_2S_4$ were re-

ported in [50]. Vapour pressure measurements were made in the temperature range 967 – 1280 K. Because the vapour pressure of $CdS(s)$ is more than 100 times of that of $Ga_2S_3(s)$, the vapour is that of $CdS(s)$, viz.Cd(g) and $S_2(g)$, by the reaction :

$$CdS(s) \rightarrow Cd(g) + 1/2S_2(g) \tag{4.9}$$

The composition of the vapour is sulfur-rich. Furthermore, presence of the vapour of $S_2(g)$ from reaction (4.9) suppresses the vaporization of $Ga_2S_3(S)$. Also it has been established that $Ga_2S_3(s)$ is characterized by a congruent evaporation process. Therefore a deviation from the stoichiometry in the resulting as-grown $CdGa_2S_4$ can only be due to the evaporation of CdS(s). Thus, the deviation from molecularity is characterized by $\delta x < 0$ and the deviation from molecularity by $\delta y < 0$.

$CdIn_2Se_4$

The vaporization behaviour and vapour pressures over samples initially $CdIn_2Se_4(s)$ were determined in the temperature range 960 – 1100 K [48]. The vaporization reactions were :

$$CdSe(ss) \rightarrow Cd(g) + 1/2Se_2(g) \tag{4.10}$$

and

$$In_2Se_3(ss) \rightarrow In_2Se(g) + Se_2(g) \qquad (4.11)$$

Contribution to total pressure by reaction (4.11) is negligible, both because CdSe(s) is more volatile than $In_2Se_3(s)$ by a factor of 40, and because of the mass action effect of the $Se_2(g)$ produced by reaction (4.10).

Thus, the deviation from molecularity is characterized by $\delta x < 0$ and the deviation from stoichiometry by $\delta y < 0$.

$ZnIn_2S_4$

This compound was studied in the temperature range from 1088 to 1218 K [51]. The vaporization reaction is :

$$ZnIn_2S_4(s) \rightarrow Zn(g) + In_2S(g) + 3/2S_2(g) \qquad (4.12)$$

the compound vaporizes congruently up to 1220 K. Above this temperature the compound vaporizes incongruently. To obtain the desired values of δx and δy, the partial vapour pressure data reported in [51] were extrapolated to higher temperatures (Fig. 4.1). Obviously, $\delta x < 0$, and $\delta y > 0$.

$ZnGa_2S_4$

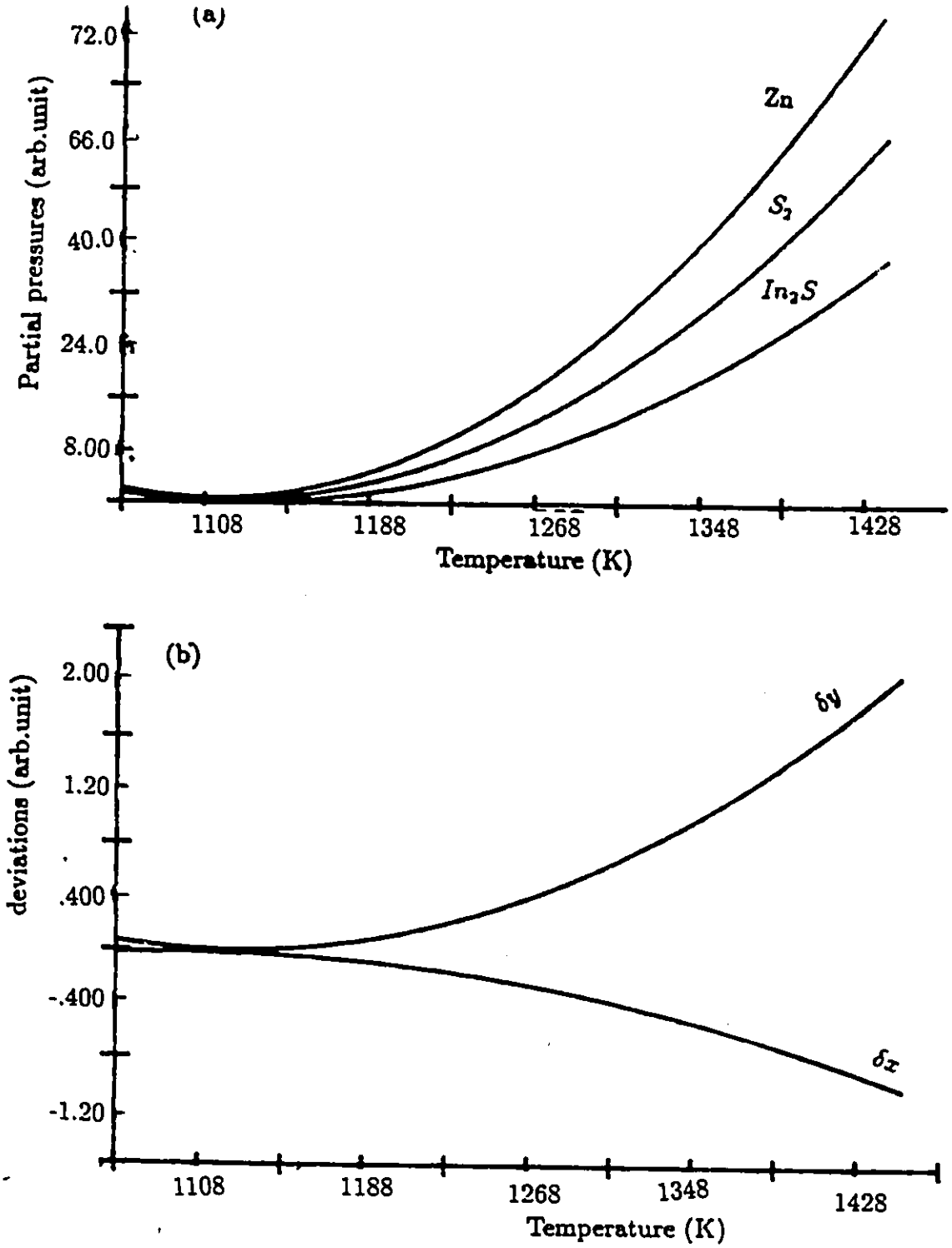

Figure 4.1: Extrapolated partial vapour pressure curves (a), and deviation from molecularity and stoichiometry (b) for $ZnIn_2S_4$.

This system was studied in the temperature range from 1106 to 1209 K [52]. Both binary constituents are significantly volatile; the vapour pressure of ZnS(s) is only $3-3.5$ times that of $Ga_2S_3(s)$. As in the case of $ZnIn_2S_4$, to obtain the desired values of δx and δy, the pressure data were extrapolated to higher temperatures (Fig. 4.2). From this figure we see that $\delta x < 0$ and $\delta y > 0$.

$PbIn_2S_4$

The vaporization study of this compound was reported in [53]. The compound was found to vaporize incongruently by :

$$PbIn_2S_4(s) \rightarrow In_2S_3(s) + PbS(g) \tag{4.13}$$

From reaction (4.13) we can tell that $\delta x < 0$ and $\delta y = 0$.

$PbGa_2S_4$

The vaporization behaviour of this compound is very complicated [17]. The vaporization produces first PbS(g) and $Ga_2S_3(s)$. Then, $Ga_2S_3(s)$ vaporizes congruently to produce $Ga_2S(g)$ and $S_2(g)$. Thus, there is no deviation from stoichiometry ($\delta y = 0$). The deviation from molecularity is characterized by $\delta x < 0$.

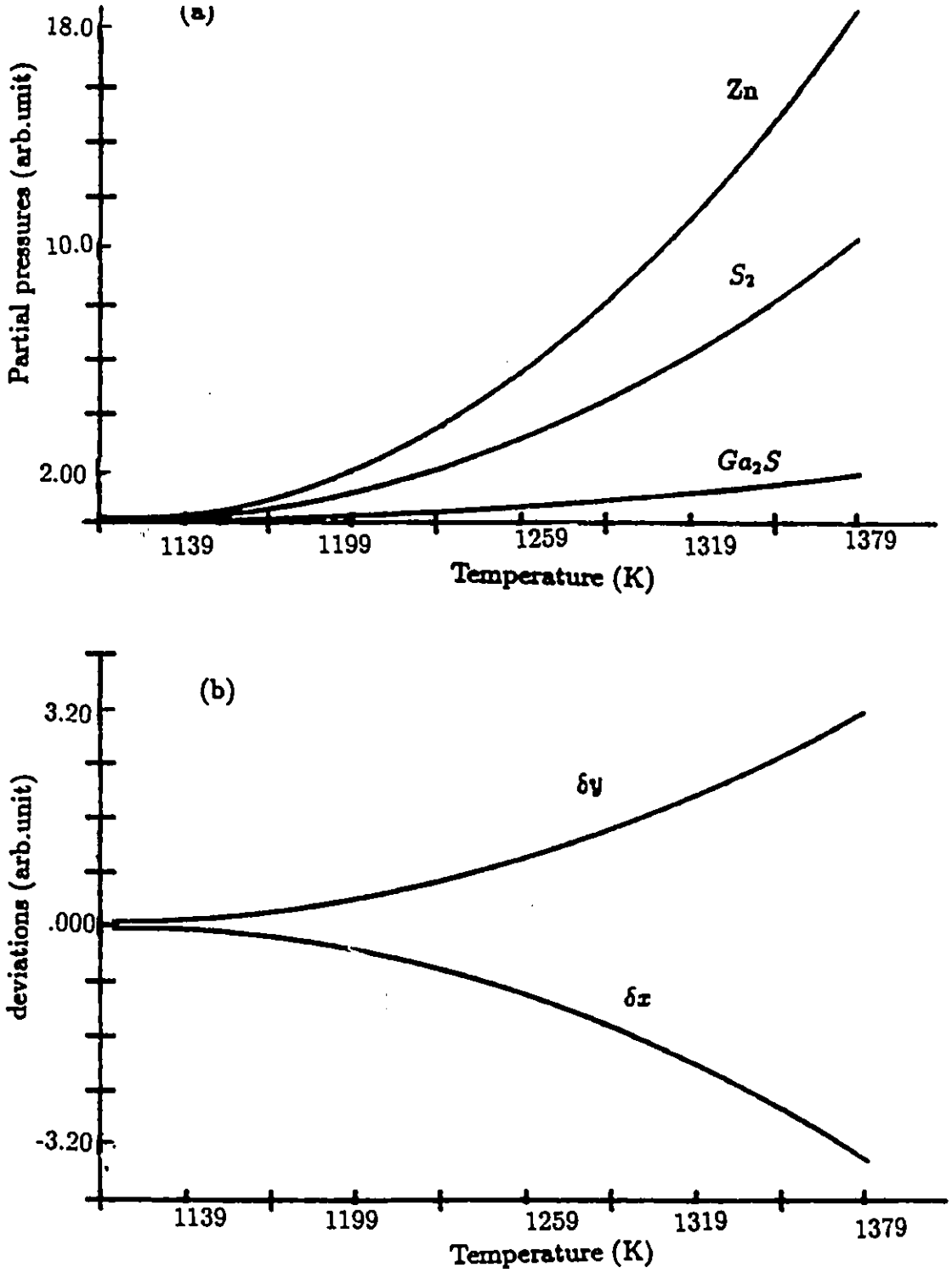

Figure 4.2: Extrapolated partial vapour pressure curves (a), and deviation from molecularity and stoichiometry (b) for $ZnGa_2S_4$.

4.4 Discussion

To facilitate the following considerations the values of δx and δy, the expected predominant intrinsic defects, and the conductivity-type are compiled in table 4.1.

First, all the compounds are characterized by $\delta x < 0$. This is so because the trivalent-metal sulfides are much more volatile than the divalent-metal sulfides. Secondly, the Cadmium compounds are characterized by a deficiency (S_2,Se_2) whereas the Zinc compounds are characterized by an excess of S_2. No stoichiometry deviation is expected for the Lead compounds. Because, to our knowledge, no electrical study has been reported for the Lead ternary compounds, we will limit ourselves to the Cadmium and Zinc compounds. It follows from all the data published in the literature that these compounds can be grown only n-type conducting. Furthermore, it has been found that as-grown single crystals have usually very high resistivities and are very compensated (donors-acceptors compensation). This is in agreement with our predictions (table 4.1) if we consider the electrical activity of the present defects in the ionic model. However, it must be noted that these predictions are not completely unambiguous; for a given

Compound	δx	δy	Intrinsic Defects	Type of Conductivity
$CdIn_2S_4$	< 0	< 0	$(In_i, V_{Cd}, In_{Cd}), V_S$	n
$CdIn_2Se_4$	< 0	< 0	$(In_i, V_{Cd}, In_{Cd}), V_{Se}$	n
$CdGa_2S_4$	< 0	< 0	$Ga_i, V_{Cd}, Ga_{Cd}, V_{Cd}$	n
$ZnIn_2S_4$	< 0	> 0	In_i, V_{Zn}, S_i	n
$ZnGa_2S_4$	< 0	> 0	Ga_i, V_{Zn}, S_i	n
$PbIn_2S_4$	< 0	$= 0$	——	intrinsic (predicted)
$PbGa_2S_4$	> 0	$= 0$	——	intrinsic (predicted)

Table 4.1: The Deviation From The Stoichiometry, The Deviation From Molecularity And Predominant Intrinsic Defects In As-grown AB_2C_4 Crystals.

δx and δy, many intrinsic defects are possible. Thus, more data is needed (especially the defects formation energies) before a final decision regarding the predominant defect can be made.

We point out the presence of V_A in all these crystals. Indeed, it has been found that the 'common' photoluminescence band in these compounds exhibits a linear relation as a function of the energy gap which indicates that the origin of this band is the same in all the compounds (a vacancy in the A sublattice) [2]. Also, it follows from table 4.1 that A_B defects, to which many optical and electrical properties have been ascribed in the literature [3], are very unlikely in these compounds provided that stoichiometric starting materials are used in the growth experiment.

The multiplicity of the observed acceptor-like centers [54] may be explained by the presence of singly and doubly charged defect centers (such as V_{Zn}^{2+} and V_{Zn}^{3+}).

Let us now look at the possibility of obtaining the inversion of the type of conductivity. It is evident that p-type conductivity due to intrinsic doping effects can be only achieved in those AB_2C_4 compounds in which the formation energy of at least one of the acceptors (V_A,C_i) is below the formation energies of the donors (V_C,B_A,B_i). All attempts to prepare p-type $AB_2(S_4, Se_4)$ by annealing in (S_2, Se_2) vapour have not been successful because this condition is not fulfilled and this is due to :

- The metalloid vapour consists mainly of molecules (S_2, Se_2) which interact weakly with the solid phase. This limits the formation of C_i centers.

- Also, and more important, the annealing leads to the formation of V_A defects (because A is a volatile element). It is clear that the V_A and the B_i centers (the latters are present because B is the less volatile element) can annihilate each other with the formation of the antistructure defects B_A (donors). So, a critical equilibrium exists between V_A, B_i, and B_A; we try to produce more acceptor centers but in the same time we can not avoid the formation of more donor centers.

The second point is particularly important for the $CdIn_2(S_4, Se_4)$ compounds because the probability of formation of antistructure defects B_A depends clearly on the similarity between the characteristics of the two cations A and B. In these two compounds the cations have identical electronegativity (1.7 ev) and almost identical ionic radii ($R_{Cd^{2+}} = .99\times10^{-8}$cm, $R_{In^{3+}} = .92\times10^{-8}$cm) [55]. Indeed, despite all the efforts made up to now, it was impossible to obtain an inversion of the type of conductivity in these

two compounds. In contrast, it is shown in [55] that the implantation of Neon ions into $ZnIn_2S_4$ and $CdGa_2S_4$ with subsequent annealing in sulfur vapour leads to p-type conductivity (this is caused by a increase of the number of the acceptor centers V_{Cd} and V_{Zn}). This fact confirms the idea that the antistructure defects are the principal obstacle in obtaining the inversion of the type of conductivity.

Strelchenko et al. [56] reported that the ternary semiconductors ABC_2 containing Se vaporize in essentially the same manner as similar compounds containing Te. If this is true also for the AB_2C_4 compounds, one can ask why it is relatively very easy to inverse the type of conductivity in $CdIn_2Te_4$ [57] whereas it was impossible to do so in $CdIn_2(S_4, Se_4)$. One explanation is that the relatively big size of Te atoms (in comparison with S and Se atoms) tends to reduce the possibility for In atoms to substitute for Cd atoms. This explanation is supported by the fact that the sulfur-rich $CdIn_2S_4$ crystals exhibit longer relaxation times at the order-disorder transition than crystals prepared with no additional S [8].

Finally, we suggest the following experiment as an attempt to inverse the type of conductivity in $CdIn_2(S_4, Se_4)$. The crystals have to be annealed in a saturated vapour of (S_2, Se_2) in the presence of $CdIn_2(S_4, Se_4)$ powder to ensure that the elemental equilibrium vapour pressures are provided during the heat treatment, mainly by the powder. We think that this will

tend to reduce the possibility for the Indium atoms to substitute Cadmium atoms. If it is the case, the diffusion of (S,Se) in the crystals will lead to the reduction of V_C population and/or the formation of interstitial defects C_i. Such method has been applied successfully to $CdSiP_2$ [58] and to $CuInSe_2$ [59].

Chapter 5

FUNDAMENTAL ABSORPTION EDGE IN $CdIn_2S_4$

5.1 Introduction

As reported in chapter 2, many investigations have been reported for the interband transitions in $CdIn_2S_4$ single crystals. These investigations include reflectivity, absorption, photoconductivity, and photovoltaic effect [20,24],

but the agreement among the data is often poor. From the theoretical point of view, band calculations agree on the existence of an indirect gap, but they disagree on the actual energy values of the different gaps. Here, we report the results of the study of the optical absorption in the range of the fundamental absorption edge.

5.2 Experimental Procedure

The samples used in this experiment were prepared as described in chapter 3 with a stoichiometric composition. The crystals were cut into plates and then polished to the desired thickness between 0.4 to 0.6 mm with an alumininum oxide polishing powder. The thickness was determined by direct measurement with a dial gauge.

The transmission spectra were measured at room temperature and at liquid N_2 temperature and in the photon energy range E = 1.5-2.8 ev. The samples were mounted in an optical cryostat. A quartz lamp was used as a light source. The light beam was passed through a Spex monochromator and chopped with a frequency of about 170 Hz. The light was then incident on the surface of the crystal which was of good optical quality. The transmission spectra were detected using a Hamamatsu (R649) photomultiplier-

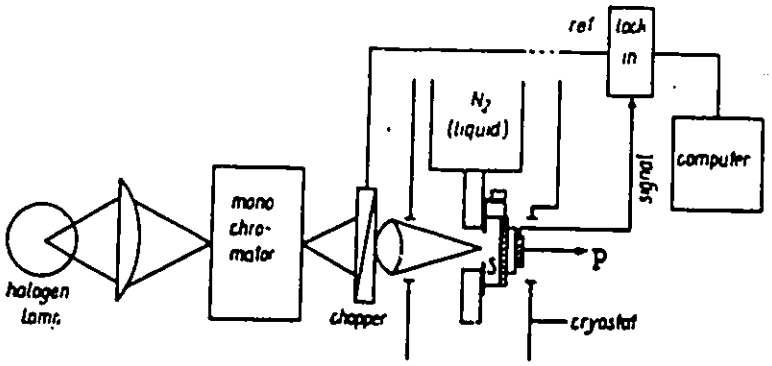

Figure 5.1: Experimental apparatus for measuring the optical absorption

detector. The signals were processed by standard synchronous techniques and then fed to a microcomputer. The measured spectra were normalized for source variations and spectral response of the optical system by dividing them by a reference spectrum measured without crystal. The data was stored in the computer with all the parameters of the measurements for subsequent analysis. A block diagram of the experimental apparatus is shown in Fig. 5.1.

5.3 Results and Discussion

Since no interference effects were observed in the spectra, the optical absorption coefficient $\alpha(\hbar\omega)$ was calculated by means of the standard relation between the transmission coefficient T, the absorption coefficient α, and reflectivity R [60],

$$T = \frac{(1-R)^2 exp(-\alpha.t)}{1-R^2 exp(-2\alpha.t)} \tag{5.1}$$

where t is the thickness of the sample. R is assumed to be independent of temperature and wavelength and equal to 0.22 [24].

Typical absorption curves are shown in Fig. 5.2 in the form of a plot of α vs. photon energy $\hbar\omega$. The absorption tails in the transparent region are due to the intrinsic defects and will be considered later. On raising the energy of illuminating light starting from about 2.00 ev, a rapid increase of the absorption coefficient is observed. The break in the $\alpha(\hbar\omega)$ curves is due to the difference of the transition types (direct/indirect) responsible for the absorption in the relevant ranges. To determine the fundamental gap energy E_g and the nature of the optical transitions involved, we tried to analyse the spectra of Fig. 5.2 in terms of the general relation [60],

$$\alpha = \frac{A}{\hbar\omega}(\hbar\omega - E_g)^n \tag{5.2}$$

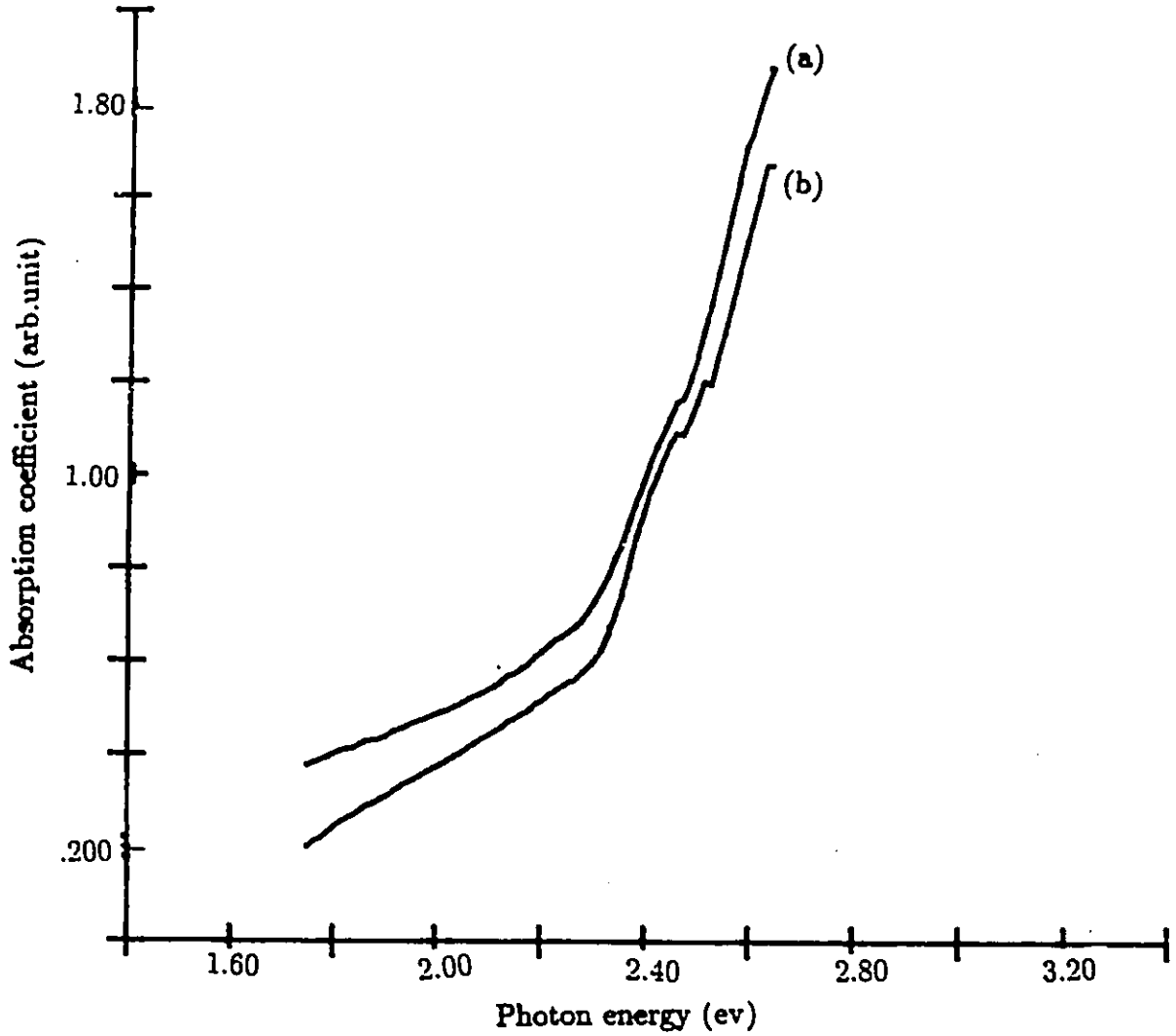

Figure 5.2: Absorption coefficient vs. photon energy for $CdIn_2S_4$ at R.T (a) and at L.N.T (b).

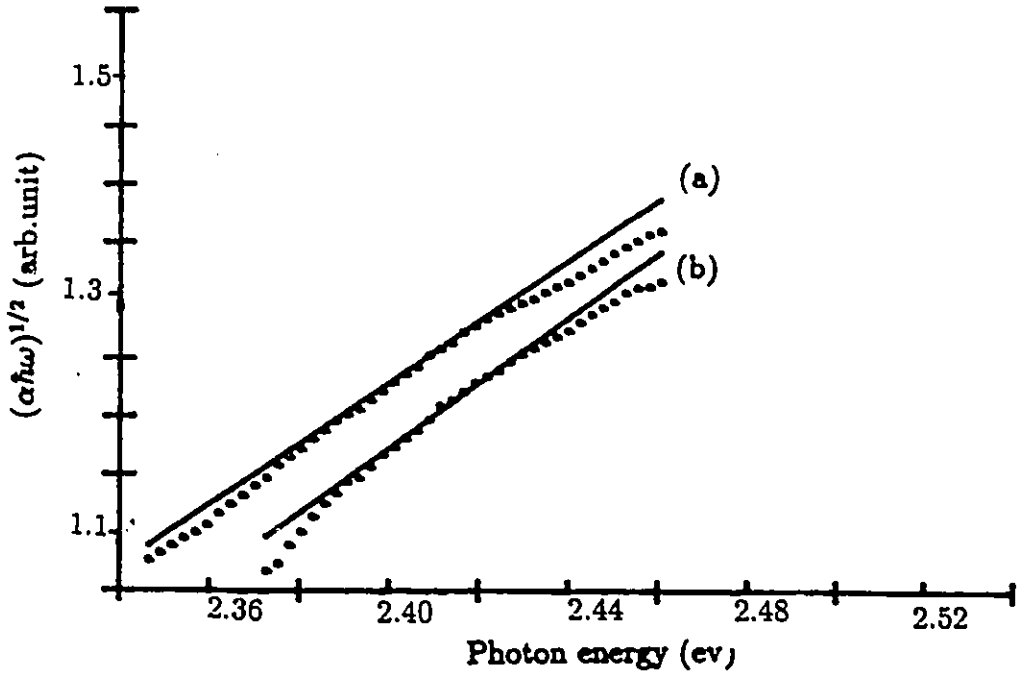

Figure 5.3: $(\alpha\hbar\omega)^{1/2}$ vs. $\hbar\omega$ plot for $CdIn_2S_4$ at R.T (a) and at L.N.T (b).

where A is a constant and the exponent n depends on the nature of transitions.

Fig. 5.3 is a reploting of Fig. 5.2 as $(\alpha\hbar\omega)^{1/2}$ vs. $\hbar\omega$ in a limited range of photon energy. It can be seen that $(\alpha\hbar\omega)^{1/2}$ varies almost lineary with $\hbar\omega$ indicating that indirect-allowed transitions prevail in $CdIn_2S_4$ in that range of energy. The corresponding gap energies E_g^i can be determined by extrapolating the $(\alpha\hbar\omega)^{1/2}$ vs. $\hbar\omega$ to zero. This gives a value of $E_g^i = 2.02ev$ at room temperature and $E_g^i = 2.12ev$ at L.N.T. with a thermal shift of about $5 \times 10^{-4} ev/K$. If we assume a linear thermal shift down to very low temperatures, this gives a value of $E_g^i = 2.18ev$ at 0K.

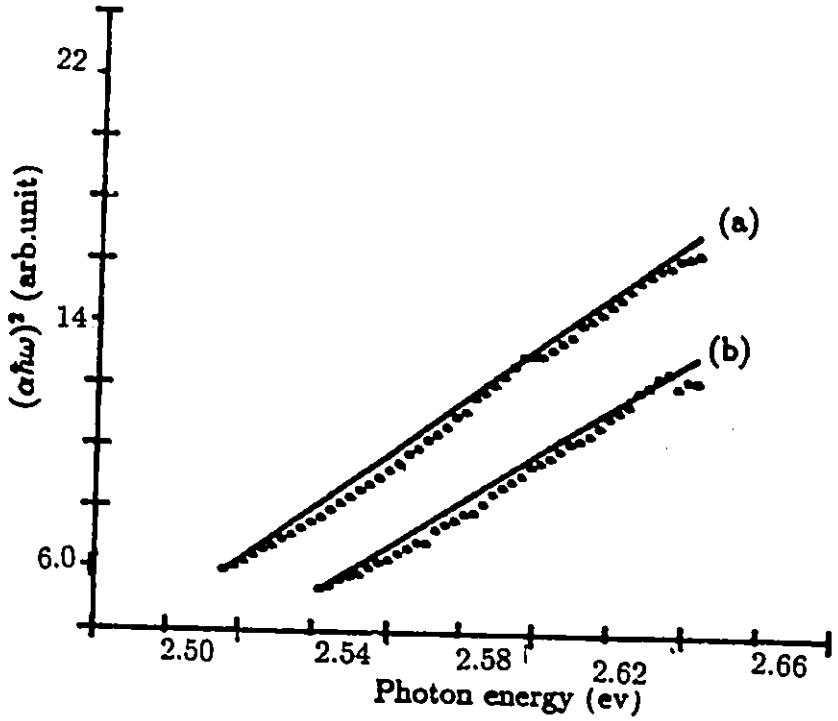

Figure 5.4: $(\alpha\hbar\omega)^2$ vs. $\hbar\omega$ plot for $CdIn_2S_4$, (a) R.T, (b) L.N.T .

At higher energies, the direct optical transitions are predominant. Fig. 5.4 shows a plot of $(\alpha\hbar\omega)^2$ vs. $\hbar\omega$ in the range of higher photon energies than those for indirect transitions. As it can be seen, nearly straight lines are obtained which, extrapolated to zero, yield the direct forbidden gap: $E_g^d = 2.41ev$ and 2.48 ev at room temperature and L.N.T respectively, with a thermal shift of about $3.5 \times 10^{-4} ev/K$ which gives a value of $E_g^d = 2.52ev$ at 0K.

In table 5.1 the values found in the present work are compared with the gap data reported in the literature. For the indirect transition at R.T a good agreement is found with Ref.[61], while the values reported in [20,62] are slightly higher (0.1ev), a notable exception is the value reported by Nakanishi [24].

At low temperature the agreement is very good with the exception of the value reported in Ref.[24] and Ref.[63]. The values for the lowest direct optical transition are spread in a wide range of energy (2.3-2.62 ev at R.T). At room temperature, our value of 2.41 ev is reasonably close to the values reported in Ref.[63] and Ref.[20]. At low temperature, our result is lower than those reported by the various workers (about 0.2 ev).

The differences in the gap data might be caused by:

	Indirect Gap(ev)		Direct Gap(ev)		
Technique	R.T.	L.T.	R.T.	L.T.	Ref.
absorption	2.02	2.12 (80K)	2.41	2.48 (80K)	this work
absorption	2.00	2.20 (77K)	2.3		[61]
absorption	2.12		2.3		[62]
absorption		2.50(0K)*	2.42	2.61(100K)	[63]
absorption		2.21 (5K)			[65]
absorption	2.28	2.44 (0K)*	2.62	2.75 (0K)*	[24]
elect.conduct.		2.20 (0K)*			[23]
PV	2.11	2.17 (100K)	2.47	2.63(100K)	[20]

Table 5.1: Values of energy gaps of $CdIn_2S_4$ according to various sources. Values followed by (*) were extrapolated assuming a linear thermal shift from R.T. down.

- Compositional variations: the $CdIn_2S_4$ and In_2S_3 form a complete solid solution and the energy gap shows a continuous change with composition [64],

- The excess or deficiency of sulfur: it is known that an annealing in sulfur vapor shifts the band edge to lower energies [66]. This may be explained by the fact that crystals grown from stoichiometry composition are degenerate whereas crystals grown with excess of sulfur are non-degenerate [23]. For a degenerate n-type semiconductor, the optical energy gap is given by the separation between the lowest unfilled level in the conduction band which lies above the bottom of this band and the corresponding level in the valence band which lies below the top of this band, and not simply by the minimum separation between the two bands.

Let us now look at the tails in the absorption edge.

Various workers have measured an exponential trap distribution over a small range of energy [24]. In our case, the absorption tail extends over an interval of almost 0.5 ev. Fig. 5.5 shows a plot of Logα vs. $\hbar\omega$ for energies below the band gap. Contrary to the usual assumption, a purely exponential trap distribution was not observed: the experimental curves, Logα=f($\hbar\omega$), deviate appreciably from straight lines at low energies, espe-

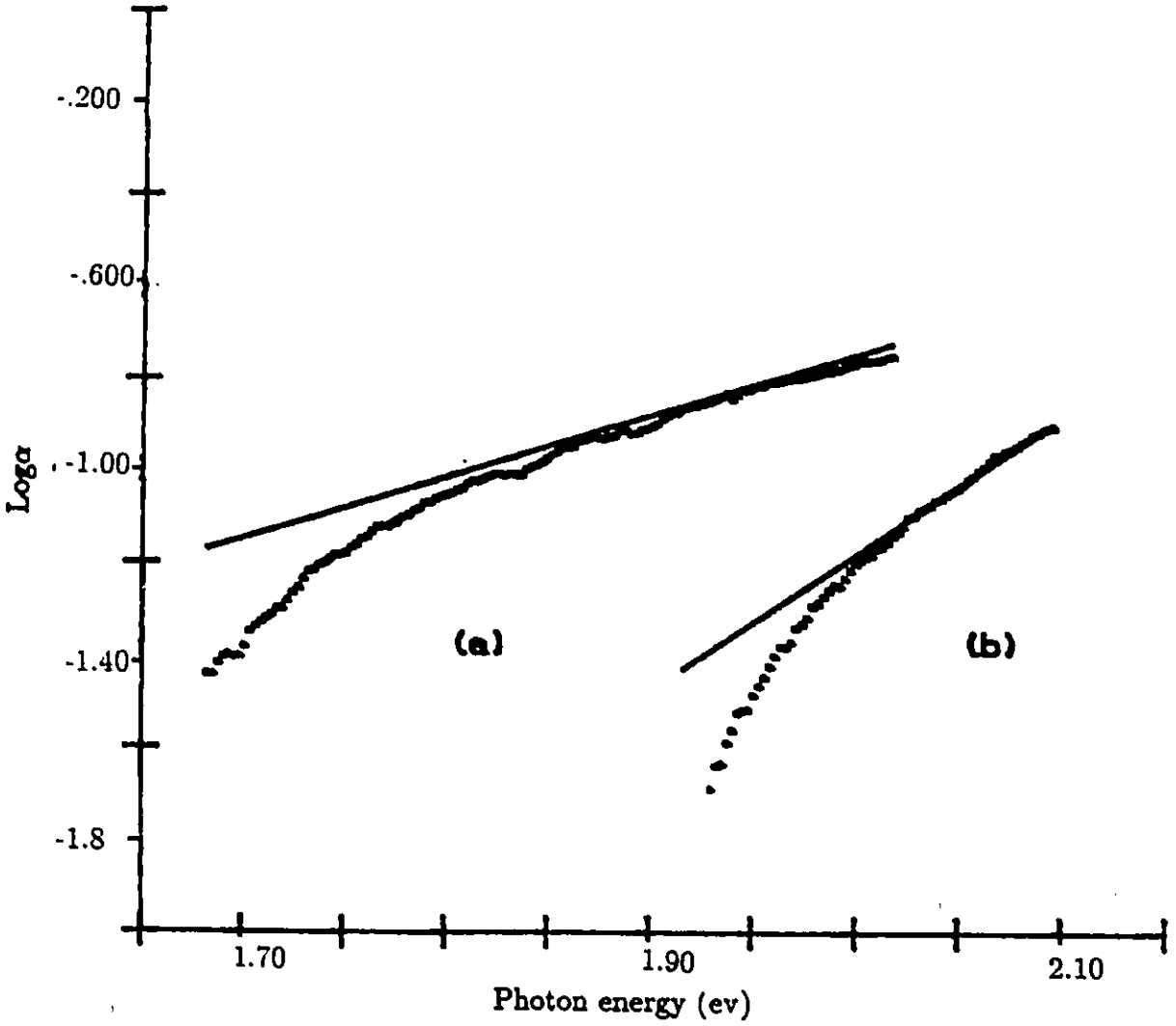

Figure 5.5: Logα vs. $\hbar\omega$ for $CdIn_2S_4$ in the range of the absorption tail, (a) R.T, (b) L.N.T .

cially at the low temperature. Cooling shifts the absorption edge toward higher energies and changes the slope of the straight lines (13/decade at R.T and 29/decade at L.N.T). This is in contradiction with the results reported in [24] where it is stated that the slope does not depend strongly on the temperature.

Now, how to explain this non-exponential dependence of the absorption coefficient on the photon energy ?. One explanation is that, if we still assume a quasi-continuous distribution of levels, their density decreases in a non-exponential way especially at the bottom of the trap distribution. Similar behavior was recently observed in $ZnIn_2S_4$ [67]. Another explanation is that the trap distribution is made of discrete levels very close to each other: the optical absorption process involves a series of different trapping levels at different energies. These levels are not resolved because of their broadening due to their high density. The latter explanation is supported by a recent study of the thermally stimulated conductivity of $CdIn_2S_4$ [25]; well defined structures in the experimental curves corresponding to three discrete levels have been found.

Chapter 6

CONCLUSIONS AND SUGGESTIONS

We undertook a study of the AB_2S_4 compounds and particularly the $CdIn_2S_4$ member of this family.

The review done in Chapter 2 reveals "regularities" in the changes of the properties of these crystals. It reveals also that studies of this family meet with considerable difficulties due mainly to the tendency of the ternary compounds to deviate from the ideal composition.

The Bridgman technique has been proved to be potentially useful for the growth of large single crystals of good optical quality. The only limitations

of this method are: the high melting points and vapour pressures of some of these semiconductors.

From Chapter 4, it can be concluded that the predominant intrinsic defects in these crystals can be derived from the expected deviation from molecularity and valence stoichiometry due to their incongruent evaporation. The electrical properties of these compounds have been explained by considering these defects in the ionic model which is reasonable for this type of crystals. The antistructure defects are the principal obstacle in obtaining the inversion of the type of conductivity. The p-type conductivity may be achieved by reducing the possibility of the A-B exchange and at the same time introducing an excess of the C element as outlined in the experiment suggested in Chapter4.

From the optical absorption data reported in Chapter 5, we found that the $CdIn_2S_4$ has an indirect-allowed gap of $E_g^i = 2.02ev$ and a direct-allowed gap of $E_g^d = 2.41ev$ (at R.T.). We can not say that our results are better than the values reported in the literature. It does point however, the difficulty in obtaining reliable values since the band gaps values are sensitive to crystal growth and crystal preparation. The absorption tail is due to the trap distribution which, according to our results, does not have an exponential form as it is generally believed. We think that either the density of these traps decreases in a non-exponential way at low energies or the trap

distribution is made of discrete levels very close to each other.

We suggest :

- To undertake a systematic study of these compound,i.e. reporting compositional analysis, optical absorption, electrical properties, as well as the extrinsic properties (PhC and PhL) on the same samples. This will reveal the relationship between these properties.

- A successful identification of the interband transitions can be done using single-crystal films and high spectral resolution techniques (for example, the modulation methods). Up to now it was difficult to obtain very thin samples just by polishing.

- To study the intrinsic defect levels inside the band gap, we suggest the use of the "double source optical absorption and photoconductivity technique" outlined in [78]; high intensity monochromatic light ensures the steady state population of the levels, and probe light of low intensity serves to measure the corresponding spectra. The experimental curves (composed of several overlapping bands) can be decomposed into individual contributions using the method developed in [78] (a program has been developed in our laboratory,i.e. DECOMP.NNLS to do this job, unfortunately we could not find time

to do this experiment).

Appendix A

Changes In Linear Susceptibility With Substitutional Variations Of Isoelectronic Elements In Non-metallic Compounds

A.1 Introduction

Recently, a relationship between the critical temperature of a superconducting compound and the position of its components in the Periodic Table was pointed out [68,69]. A similar relationship was also mentioned for the band gap of non-magnetic semiconductors [34]. In the later case, it was found that the change in E_g for isoelectronic substitution of one of the elements in the compound was either positive or negative depending on the value of N, the number of its outer electrons. This phenomena was qualitatively related to the filling of closed electrons shells around the core.

Since the refractive index plays an important role in many physical processes [70,75] and often has to be considered in the evaluation of a material for engineering purposes, it was of interest to determine if some useful relationship could not be also found for that parameter. Already, some general criteria as how the index varies as a function of element position in the periodic chart have been useful in regard to choosing specific multinary compounds for particular applications [70]. Furthermore,many attempts have been made to find a general relation between the refractive index and the band gap of which Moss'and Ravindra's formulas are the better known [71]. One can think that, using these formulas along with the previously mentioned relationship between the E_g and the position of the components

in the Periodic Table [34] could make the equivalent relationship for the refractive index redundant. This is not the case since we found that the relationship that holds for the refractive index can be expressed in a much simpler form and is more readily compared to existing dielectric theory of crystals [35].

A.2 Discussion

The parameter of interest in this work is n_0, the zero frequency refractive index defined by:

$$n_0 = 1 + \frac{1}{2\pi^2} \int K d\lambda \qquad \text{(A.1)}$$

where K is the absorption coefficient. Table A.1 lists the values of n_0 for a large variety of semiconducting and insulating compounds [70,76,77]. The table is arranged in sub-groups, each sub-group corresponding to compounds varying only by the substitution of one isoelectronic element. The parameter N is the number of outer electrons of the substituted element and so corresponds to the column number in the Periodic Table. No special attention is paid to the crystal structure or the number of elements forming the compound. In some cases, n_0 was not available but ε_∞ was and we have used the approximation: $n_0 = \sqrt{\varepsilon_\infty}$ to calculate n_0. When this

approximation is used for a particular element, it is also used for the rest of the elements of that sub-group. Finally, since we had so little data on transition elements substitution to be of statistical significance, entries for $N = 4$ to $N = 10$ were left out. This also avoids discussing any element with an unfilled d-shell.

Chapnik [68,34] has used similar tables to define relationships between E_g and T_c vs. N. We preferred expressing our relationship in a more quantitative way. For that purpose, we have plotted the function $\frac{2\Delta n_0}{(\bar{n_0}-\bar{n_0}^{-1})}$ vs. N (Fig A.1), where Δn_0 is the change in the refractive index when two isoelectronic elements from neighboring rows of the Periodic Table are exchanged, and $\bar{n_0}$ is their average refractive index. This particular functional was chosen to allow easy comparison with the PV dielectric theory [72] which is expressed in terms of the linear electric susceptibility as:

$$\frac{\Delta\chi}{\chi} = \frac{2\Delta n_0}{n_0 - n_0^{-1}} \tag{A.2}$$

Some remarks concerning Fig A.1 are in order. This graphically represents the average change in refractive index as a function of N, calculated from 141 data points reported in table A.1 and using equation(A.2). The vertical bars represent estimates of standard deviations calculated assuming a normal distribution. However, Fig. A.2 shows clearly that Δn_0 does not follow a normal distribution but is skewed toward positive changes in the

N=1		$CuGaS_2$	2,50	BP	2,8	$SiCdAs_2$	3,5	N=16		S_2GaCu	2,49
		$AgGaS_2$	2,41	AlP	2,8	$GeCdAs_2$	3,56			Se_2GaCu	2,8
LiF	1,38			GaP	2,9	$SnCdAs_2$	3,70	OSr	1,87	Te_2GaCu	3,3
NaF	1,30	$CuGaTe_2$	3,3	InP	3,1			SSr	2,09		
KF	1,34	$AgGaTe_2$	3,3			$SiZnAs_2$	3,1	SeSr	2,21	S_2GaAg	2,4
RbF	1,38			AlSb	3,19	$GeZnAs_2$	3,5	TeSr	2,4	Se_2GaAg	2,18
		$CuInTe_2$	2,58	GaSb	3,79	$SnZnAs_2$	3,6	S	2,04	Te_2GaAg	3,3
LiCl	1,64	$AgInS_2$	2,50	InSb	3,95			Se	2,45		
NaCl	1,52					N=15		Te	5,3	S_2InCu	2,58
KCl	1,48	$CuInTe_2$	3,4	$AlCuS_2$	2,40					Se_2InCu	2,9
RbCl	1,48	$AgInTe_2$	3,4	$GaCuS_2$	2,50	NB	2,1	BeO	1,73	Te_2InCu	3,4
				$InCuS_2$	2,58	PB	2,8	BeS	2,60		
LiBr	1,79	$CuGaSe_2$	2,8			AsB	3,2	BeSe	2,91	S_4Tl_3As	2,83
NaBr	1,61	$AgGaSe_2$	2,63	$AlCuSe_2$	2,6			BeTe	2,90	Se_4Tl_3As	3,3
KBr	1,52			$GaCuSe_2$	2,8	NaI	2,16				
RbBr	1,55	N=12		$InCuSe_2$	2,9	PAl	2,75	OMg	1,71	N=17	
						AsAl	3,00	SMg	2,27		
LiI	1,95	ZnO	1,92	$AlCuTe_2$	3,3	SbAl	3,19	SeMg	2,40	ClCs	1,61
NaI	1,73	CdO	2,32	$GaCuTe_2$	3,3			TeMg	2,80	BrCs	1,67
KI	1,64	HgO	2,45	$InCuTe_2$	3,4	NGa	2,4			ICS	1,82
RbI	1,64					PGa	2,90	OCa	1,81		
		ZnS	2,27	Ga_2CdS_4	2,30	AsGa	3,3	SCa	2,13	FNa	1,30
N=2		CdS	2,38	In_2CdS_4	2,55	SbGa	3,79	SeCa	2,25	ClNa	1,52
		HgS	2,67					TeCa	2,50	PrNa	1,61
BeO	1,73			N=14		NIn	2,56			INa	1,73
MgO	1,71	ZnSe	2,43			PIn	3,1	OZn	1,92		
CaO	1,81	CdSe	2,49	C	2,35	AsIn	3,5	SZn	2,27	ClCu	1,93
SrO	1,87			Si	3,46	SbIn	3,95	SeZn	2,43	BrCu	2,116
BaO	1,98	ZnTe	2,70	Ge	4,0			TeZn	2,7	ICu	2,346
		CdTe	2,70	Sn	4,8	As_2S_3	2,66				
BeS	2,60	HgTe	3,74			Sb_2S_3	2,73	OCd	2,32	$ClNaO_3$	1,50
MgS	2,27			SiO_2	1,92			SCd	2,38	$BrNaO_3$	1,60
CaS	2,13	Zn_3As_2	3,85	SnO_2	2,0	P_2ZnSi	3,1	SeCd	2,49		
SrS	2,09	Cd_3As_2	5,75			As_2ZnSi	3,1	TeCd	2,7	FLi	1,38
BaS	2,10	$ZnSiP_2$	3,1	GeS	3,4					ClLi	1,64
		$CdSiP_2$	3,1	SnS	4,4	P_2CdSi	3,1	OPb	2,56	BrLi	1,79
BeSe	2,91					As_2CdSi	3,5	SPb	4,15	ILi	1,95
MgSe	2,40	$ZnSnP_2$	2,9	GeTe	6,0			SePb	4,74		
CaSe	2,25	$CdSnP_2$	3,1	SnTe	6,7	P_2ZnSn	2,9	TePb	5,3	FK	1,34
SrSe	2,21					As_2ZnSn	3,6			ClK	1,48
		$ZnGeP_2$	3,13	$SiCdP_2$	3,1			OSn	4,4	BrK	1,52
BeTe	2,9	$CdGeP_2$	3,21	$GeCdP_2$	3,21	P_2ZnGe	3,1	SSn	4,79	IK	1,64
MgTe	2,8			$SnCdP_2$	3,1	As_2ZnGe	3,5	TeSn	6,7		
CaTe	2,5	N=13								Frb	1,38
SrTe	2,4			$SiZnP_2$	3,1	PTl_3Se_4	3,09	S_2AlCu	2,4	ClRb	1,48
		BN	2,10	$GeZnP_2$	3,13	$AsTl_3Se_4$	3,3	Se_2AlCu	2,6	BrRb	1,55
N=11		AlN	2,16	$SnZnP_2$	2,9			Te_2AlCu	3,3	IRb	1,64
		GaN	2,40								
Cu_2O	2,56	InN	2,56								
Ag_2O	2,75										

Table A.1: Refractive index for groups of compounds, where N is the number of the outer electrons of the substituted element.

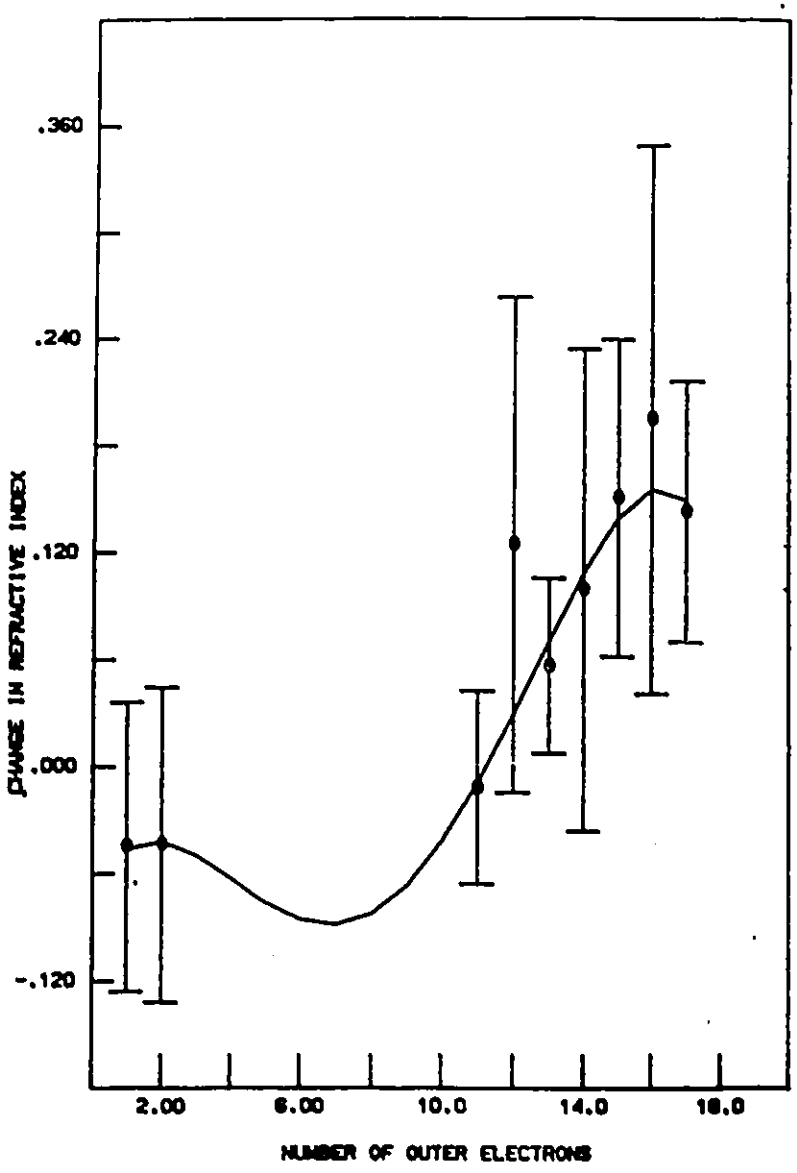

Figure A.1: Change in the refractive index (i.e, $\Delta\chi/\chi$) with isoelectronic substitution of elements as a function of the number of outer electrons of the substituted element

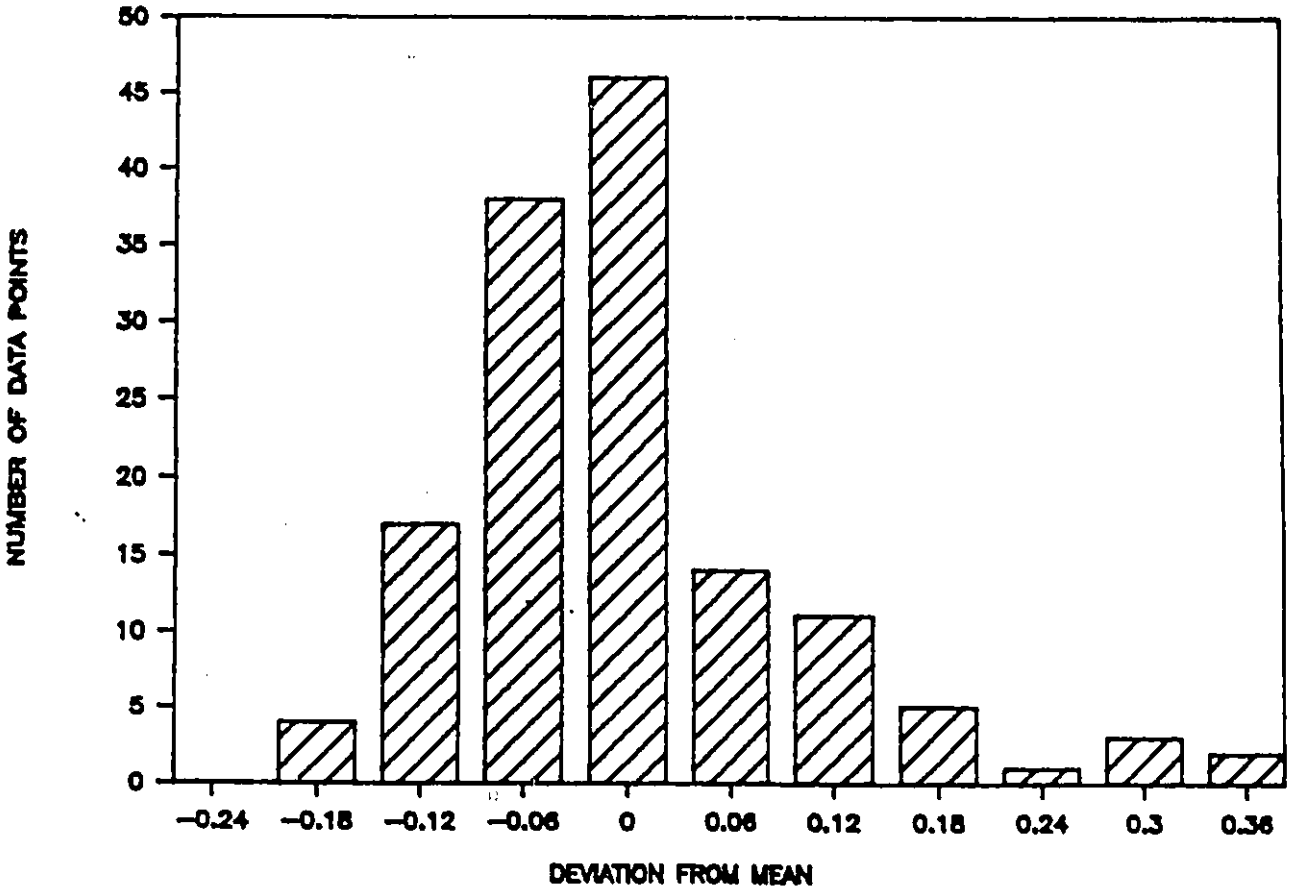

Figure A.2: Histogram of the data derived from table A.1 and illustrated in Fig. A.1. Vertical scale: No. of isoelec.subst. pairs of compounds. Horizontal scale: change in refrac.index minus the mean change for the sub-group.

refractive index. Finally, let us mention that although the solid line of Fig A.1 was obtained from a weighted least square fit to a second order polynomial, it is only provided as an indication of the trend. Specifically, we do not pretend it is of value for $3 < N < 11$ region.

The concept of crystal ionicity and in particular the dielectric description of ionicity developed by Phillips and Van Vechten [72,73] provides a suitable frame to interpret the trend revealed in Fig A.1. However, for complex compounds of varying multiplicity and crystal structure the extension of Levine [74] is more appropriate. In this case, the bond is considered to be the important constitutive element of the compound. In particular, if the crystal is composed of different types of bonds (labeled u) then the total susceptibility can be resolved into contributions χ^u from the various types of bonds,

$$\chi = \sum_u F^u \chi^u \tag{A.3}$$

where F^u is the fraction of bond of type u composing the crystal. We now make the approximation that isoelectronic substitution affects only one of these bond type so it is sufficient to consider its effect on χ^u.

Following Levine [74] we can write,

$$\chi^u = \frac{1}{4\pi}\frac{(h\Omega_p^u)^2}{(E_g^u)^2} = \frac{1}{4\pi}\frac{(h\omega_p^u)^2 D^u A^u}{E_h^2 + C^2} \tag{A.4}$$

where $\hbar\omega_\rho^u$ is the plasma frequency, E_h and C are the homopolar and heteropolar components of the effective energy gap, respectively, A^u is a small correction term introduced from the Penn model and neglected from now on, and D^u accounts for the effect of the d-state core. Furthermore,

$$C^2 \simeq E_h^2 \frac{(b\Delta z)^2}{23} \tag{A.5}$$

where b is the important correction factor related to the screening of the ion core by the outer electrons. From (A.4) and (A.5), we have the change in susceptibility,

$$\frac{\Delta\chi^u}{\chi^u} = \frac{\Delta(\hbar\omega_\rho)^2}{\hbar\omega_\rho^2} + \frac{\Delta D}{D} + \frac{2\Delta(1/E_h)}{1/E_h} - 2\bar{f}_i\frac{\Delta b}{b} \tag{A.6}$$

where $\bar{f}_i$ is the average fractional ionicity of the bond. Now, if the change is due to isoelectronic substitution, it is more convenient to use:

$$(\hbar\omega_\rho)^2 \quad \alpha \quad d^{-3}; E_h \quad \alpha \quad d^{-2.5} \tag{A.7}$$

where d is the bond length. Combining equations (A.7) and (A.6) we finally arrive at;

$$\frac{\Delta n}{n - n^{-1}} = \frac{\Delta D}{2D} + \frac{\Delta d}{d} - \bar{f}_i\frac{\Delta b}{b} \tag{A.8}$$

For very ionic bonds, Van Vechten [73] has shown that $\frac{\Delta b}{b} \sim 2\frac{\delta d}{d}$ and furthermore, for $N = 1$ and 2, the first term of equation (A.8) does not apply since there are no d electrons. Thus,

$$\frac{\Delta n}{n - n^{-1}} \simeq (1 - 2\bar{f}_i)\frac{\Delta d}{d} \simeq -0.8\frac{\Delta d}{d} \tag{A.9}$$

Equation (A.9) not only predicts the right sign for the change in the refractive index but also predicts the right magnitude of this change since an average value of 10% is reasonable for $\Delta d/d$.

For $N > 10$, all terms of equation (A.8) must be considered. Because of the added contribution of the d-electrons ($\Delta D/D \sim +10\%$), we can expect the change in refractive index to be positive with a maximum value of approximately 20% when $\bar{f}_i \sim 0$. Also, since f_i is not constant for isoelectronic substitution, the last term of equation (A.8) certainly contributes to the fairly large spread in the Δn distribution.

A.3 Conclusion

Analyzing the change in refractive index with isoelectronic substitution, a statistically significant trend is observed. The change is negative for $N < 4$ and positive and increases with N for $N > 10$. From the PV dielectric theory of crystals, one sees that changes in the screening factor are responsible for the negative Δn when $N < 4$ while d-state core electrons contribution and the increases in bond length can account for the positive Δn when $N > 10$. The large spread in Δn distribution function probably reflects the fact that the ionicity factor is not constant for isoelectronic substitution.

The results reported here and in Ref.[34] can be useful in regard to choosing specific isoelectronic substitutions to obtain multinary compounds with particular properties.

Bibliography

[1] S.I. Radautsan, A.N. Georgobiani, and I.M. Tiginyanu, Proc.Internat.Conf.Ternary Multinary Compounds, 5th, Caracas, Prog.Crystal Growth Charact. 10, 403(1985).

[2] M. Guzzi and E. Grilli, Mater.Chem.Phys. 11, 295(1984).

[3] A.N. Georgobiani, S.I. Radautsan, and I.M Tiginyanu, Soviet Phys.Semicond. 19, 121(1985).

[4] H. Hahn, G. Frank, W. Klinger, and G. Storger, Z.Anorg.Allg.Chem. 279, 241(1955).

[5] A. Miller, A. MacKinnon, and D. Weaire, Solid State Phys. 36, 119(1981).

[6] L.I. Berger and V.D. Prochukhan, Ternay Diamond-like Semiconductors (Consultants Bureau, New York, 1969).

[7] H. Haeuseller and W. Kwarteng-Acheampong, J.Sol.Stat.Chem. 72, 324(1988).

[8] W. Czaja, Phys.Kondens.Mater. 10, 299(1970).

[9] N.V. Joshi, Phys.Chem.Solids 41, 943(1980).

[10] H.V. Philipsborn, Z.Kristallogr. 133, 464(1971).

[11] J.a. Beun, R. Nitsche, and M. Lichtensteiger, Physica 26, 647(1960) and Physica 27, 448(1961).

[12] L. Suchow and N.R. Stemple, J.Electrochem.Soc. 111, 191(1964).

[13] A.L. Gentile and O.M. Stafsudd, Mater.Res.Bull. 4, 869(1969).

[14] W.A. Shand, J.Crystal Growth 5, 203(1969).

[15] O.P. Derid, Investigation of Complex Semiconductor Compounds, Shtiintsa, Kishinev, pp.44-64.

[16] G.A Busch, Nuovo Cimento Suppl. 7, 696(1958).

[17] J.G. Edwards, High Temp.Sci. 19, 93(1985).

[18] S.M. Patel M.H. Ali, Mater.Letter. 5, 350(1987).

[19] R. Horiba, H. Nakanishi, S.Endo, and T. Irie, Surf.Science 86, 498(1979).

[20] A. Anedda and E. Fortin, J.Phys.Chem.Solids 40, 653(1979).

[21] A.B. Vincent, C.E. Rodriguez, and N.V. Joshi, Can.J.Phys. 62, 883(1984).

[22] A. Baldereschi, F. Muloni, F. Aymerich, and G.Mula, Inst.Phys.Conf.Ser. 35, 193(1977).

[23] S. Endo and T. Irie, J.Phys.Chem.Solids 37, 201(1976).

[24] H. Nakanishi, Jpn.J.Appl.Phys. 19, 103(1980).

[25] T. Takizawa and K. Kanbara, J.Phys.Soc.Japan 55, 3503(1986).

[26] S. Charbonneau and E. Fortin, Phys.Rev.(B) 31, 2326(1985).

[27] A.N Georgobiani, A.N. Gruzintsev, S.A. Ratseev, I.M. Tiginyanu, and V.V. Ursaki, Cryst.Res.Technol. 21, 259(1986).

[28] S. Charbonneau, E. Fortin, and J. Beauvais, Can.J.Phys. 65, 204(1987).

[29] Y. Seki, S. Endo, and T. Irie, Jpn.J.Appl. Phys. 19, 1667(1980).

[30] C. Paorici, C. Pelosi, N. Romeo, G. Sberveglieri, and L. Tarricone, Phys.Stat.Sol.(a) 36, K33(1976).

[31] J. Beauvais and E. Fortin, J.Appl.Phys. 62, 1349(1987).

[32] K. Yamashita, H. Kasahara, K. Yamamoto, and K. Abe, Jpn.J.Appl.Phys. 21, Suppl. 21-3, 107(1981).

[33] C. Razzetti, P.P. Lottici, and G. Amtonioli, Prog.Crystal Growth Charact. 15, 43(1987).

[34] I.M. Chapnik, Phys.Stat.Sol.(b) 137, K95(1986).

[35] P. Bernard and M. Golea, Submitted to Phys.Stat.Sol.

[36] L. Tarricone, L. Zanotti, and J. Filipowicz, J.Phys.D: Appl.Phys. 20, 653(1987).

[37] E. Grilli and M. Guzzi, Phys.Stat.Sol.(a) 103, 291(1987).

[38] J.B. Mullin, in: Crystal Growth and Characterization, Eds. R. Ueda and J.B. Mullin (North-Holland, Amesterdam, 1975).

[39] J.C. Brice, The Growth of Crystals from Liquids (North-Holland, Amesterdam, 1973).

[40] H.D. Lutz, W.W. Bertram, B. Oft, and H. Haeuseter, J.Sol.Stat.Chem. 46, 56(1983).

[41] H. Haupt and K. Hess, Inst.Phys.Conf.Ser. 35, 5(1977).

[42] F.A. Kroger and H.J. Vink, Solid State Phys. 3, 307(1956).

[43] J.A. Groenink and P.H. Janse, Z.Physik.Chem.Neue Folge, Bd.110, 17(1978).

[44] B.R. Pamplin, T. Kiyosawa, and K. Masumoto, Prog.Crystal Growth Character. 1, 331(1979).

[45] H. Schmalzried and C. Wagner, Z.Physik.Chem.Neue Folge 31, 1983(1962).

[46] H. Neumann, Crystal Res.Technol. 18, K8(1983).

[47] H. Neumann, Crystal Res.Technol. 18, 483(1983).

[48] R.S. Srinivasa, H.B. Thompson, and J.G. Edwards, J.Electrochem.soc. 134, 1818(1987).

[49] S.T. Kshirsagar, H.B. Thompson, and J.G. Edwards, J.Electrochem.Soc. 129, 1835(1982).

[50] J.G. Edwards and S.T. Kshirsagar, Thermochim.Acta 59, 81(1982).

[51] J.G. Edwards R. Haque, and A.H. Qusti, Thermochim.Acta 62, 197(1983).

[52] A.S. Gates and J.G. Edwards, J.Phys.Chem. 82, 2789(1978).

[53] R. Haque, A.S. Gates, and J.G. Edwards, J.Chem.Phys. 73, 6301(1980).

[54] A. Serpi, J.Phys.D:Appl.Phys. 9, 1881(1976).

[55] A.N. Georgobiani and I.M. Tiginyanu, Soviet Physics-Lebedev Institute Reports, 2, 25(1984).

[56] S.S. Strelchenko, S.A. Bondar, A.D. Molodyk, L.I. Berger, and A.E. Balanevskaya, Neorg.Mater. 5, 593(1969).

[57] S. Kianian, S.A. Eshraghi, O.M. Stafsudd, and A.L. Gentile, J.Appl.Phys. 62, 1500(1987).

[58] A. Sodeika, Z. Silevicius, Z. Januskevicius, and A. Sakalas, Phys.Stat.Sol.(a) 69, 491(1982).

[59] J. Parkes, R.D. Tomlinson, and M.J. Hampshire, J.Cryst.Growth 20, 215(1973).

[60] J.I. Pankove, Optical Processes in Semiconductors (Prentice-Hall, Englewood Cliffs, 1971).

[61] S.I. Radautsan, I.P. Malodyan, N.N. Syrbu, V.E. Tezlevar, and M.A. Shipitke, Phys.Stat.Sol.(b) 49, K175(1972).

[62] G.B. Abdullaev, D.A. Guseinova, T.G. Kerimova, and R.Kh. Nani, Soviet Phys.Semicond. 8, 785(1974).

[63] H. Nakanishi, S. Endo, and T. Irie, Jpn.J.Appl.Phys. 12, 1646(1973).

[64] H. Nakanishi, S. Endo, and T. Irie, Proc.Conf.Ternary Multinary Compounds, 4th, Tokyo, 1980; Jpn.J.Appl.Phys. 19, 261(1981).

[65] K. Yamamoto, T. Murakawa, Y. Ohbayashi, J. Shinizu, and K. Abe, J.Phys.Soc.Japan 35, 1258(1973).

[66] A.N. Georgobiani, S.A. Ratseev, I.M. Tiginyanu, V.E. Tezlevan, and V.V. Ursaki, Soviet Physics-Lebedev Institute Reports 10, 41(1985).

[67] D.C. Randles and E. Fortin, Phys.Stat.Sol.(a) 95, K47(1986).

[68] I.M. Chapnik, Phys.Letters A109, 69(1985).

[69] I.M. Chapnik, Phys.Stat.Sol.(b) 130, K179(1985).

[70] R. Feigelson, Jpn.J.Appl.Phys. 19 ,371(1980).

[71] T.S. Moss, Phys.Stat.Sol.(b) 131, 415(1985).

[72] J.C. Phillips, Rev.Mod.Phys. 42, 317(1970).

[73] J.A. Van Vechten, Phys.Rev. 182, 891(1969).

[74] B.F. Levine, J.Chem.Phys. 59, 1463(1973).

[75] B.O. Seraphin, Optical Properties of Solids, New Developments. North Holland Publ.Co., Amsterdam 1976.

[76] V.P. Gupta and N.M. Ravindra, Phys.Stat.Sol.(b) 100, 715(1980).

[77] Landolt-Bornstein, Numerical Data and Functional Relationship in Science and technology, New Series, Ed. K.H. Hellwege and O.Madelung, Vol.17/III, Springer-Verlag, Berlin 1982/1985.

[78] J. Pastrnak, Czech.J.Phys.B 37, 933 and 942(1987).

UNIVERSITÉ D'OTTAWA
UNIVERSITY OF OTTAWA